Sustainable Cities and Society 79 (2022) 103709

Contents lists available at ScienceDirect

Sustainable Cities and Society

journal homepage: www.elsevier.com/locate/scs

Resilience-Oriented Planning of Multi-Carrier Microgrids under Cyber-Attacks

Mahdi Azimian [a,*], Vahid Amir [a], Saeid Javadi [a], Soheil Mohseni [b], Alan C. Brent [b,c]

[a] Department of Electrical and Computer Engineering, Kashan Branch, Islamic Azad University, Kashan, Iran
[b] Sustainable Energy Systems, School of Engineering and Computer Science, Wellington Faculty of Engineering, Victoria University of Wellington, Wellington 6140, New Zealand
[c] Department of Industrial Engineering and the Centre for Renewable and Sustainable Energy Studies, Stellenbosch University, Stellenbosch 7600, South Africa

ARTICLE INFO

Keywords:
Cyber-attacks
Distributed energy resources
Economic analysis
Multi-carrier microgrid
Planning
Resilience

ABSTRACT

Microgrids are inherently subject to a variety of cyber-physical threats due to potential vulnerabilities in their cyber systems. In this context, this paper introduces a cyber-attack-resilient design of a multi-carrier microgrid to avoid the loss of critical loads. The objective of the proposed model is to minimize the total planning cost of multi-carrier microgrids, which incorporates the investment and replacement costs of distributed energy resources, operation and maintenance costs, peak demand charges, emission costs, unserved energy costs, and potential reinforcement costs to handle cyber-physical attacks. Not only is the proposed multi-carrier microgrid planning approach able to determine the optimal size of multi-carrier microgrids, but it also identifies and reinforces the system to handle cyber-physical attacks by serving critical loads. The proposed multi-carrier microgrid planning model is formulated as a mixed-integer programming problem and solved using the GAMS 24.1 software. To evaluate the effectiveness of the proposed integrated resource planning model, it is applied to a real-world industrial park test-case system. Numerical simulations demonstrate the effectiveness of the resilience-oriented multi-carrier microgrid planning model. Importantly, the simulation results indicate the economic viability of multi-carrier microgrids optimized by the proposed model. Also, the model sensitivity of various decision variables has been analyzed.

1. Introduction

The term resilience refers to a system's ability to prepare for and adapt to changing conditions, as well as withstand and recover rapidly from either extreme natural disasters or human-triggered events (Mishra, Anderson, Miller, Boyer & Warren, 2020, Mishra, Ghadi, Azizivahed, Li & Zhang, 2021; Venkataramanan, Srivastava, Hahn & Zonouz, 2019). In the energy provisioning context, microgrids (MGs) are increasingly recognized as a means to improve the overall power system resilience to major power outages. The associated deployment of information and communications technologies to enable MGs improves the overall electric power systems' operational performance and reduces its vulnerability to cyber-attacks (Jimada-Ojuolape & Teh, 2020). That is, although MGs – defined as a single controllable entity integrating a potentially large number of supply-side resources in a consistently decentralized way – are generally used as resilient and reliable electricity provision solutions (Das, Munikoti, Natarajan & Srinivasan, 2020), they are vulnerable to cybersecurity-related incidents (Bajwa, Mokhlis, Mekhilef & Mubin, 2019; Cagnano, De Tuglie & Microgrids, 2020; Wang et al., 2018). Thus, it is vital to identify the associated risk factors and cyber vulnerabilities, and subsequently reinforce MGs against physical, communication, and cybersecurity-related threats. To this end, a cost-effective planning model incorporating preventive reinforcement strategies is required to ensure the financial feasibility of MG developments as truly resilient, reliable, and durable solutions against 'low-probability, high-impact' events.

A rich literature on the different methodologies used in long-term MG planning optimization already exists. For instance, the optimal formulation of an isolated MG incorporating direct load control demand response programmed is derived in Mohseni, Brent and Burmester, (2019) using a specifically developed metaheuristic optimization method. The model ensures the power reliability of a remote community by introducing a new reliability index. The study in Nagapurkar and Smith, (2019) focuses on the techno-economic feasibility and greenhouse gas minimization of a small residential community MG.

* Corresponding author.
E-mail addresses: mahdi.azimian1991@gmail.com (M. Azimian), v.amir@iaukashan.ac.ir (V. Amir).

https://doi.org/10.1016/j.scs.2022.103709
Received 15 May 2021; Received in revised form 25 December 2021; Accepted 17 January 2022
Available online 19 January 2022

Nomenclature

Indices

boiler	index for gas boiler unit
chp	index for combined heat and power unit
d	index for days
ehp	index for electric heat pump unit
electro	index for electrolyzer unit
ess	index for electrical storage unit
fc	index for fuel cell unit
h	index for hours
hss	index for hydrogen storage unit
l	index for carrier comprising {e: electricity, t: heat}
pv	index for photovoltaic unit
s	index for seasons
tss	index for thermal storage unit
u	index for distributed energy resources
wt	index for wind turbine unit
y	index for years
$\sim$	index for forecasted parameters

Sets

G	set of dispatchable units
S	set of storage system units
W	set of non-dispatchable units (wind and solar)

Parameters

A	availability coefficient of units
$Bud^{attacker}$	attacker's available budget
CC	capital cost of distributed generations
$CCr(r)$	capital replacement cost of distributed generations
CE	capital cost of storage media – energy
$CEr(r)$	capital replacement cost of storage media – energy
CIF	capital investment fund of the project
CP	capital cost of storage media – power
$CPr(r)$	capital replacement cost of storage media – power
$CR(\varepsilon)$	capital reinforcement (encryption) cost of units as a function of encryption strength
D	load demand
DOD	depth of discharge of storage media
E^{cap}	allowable energy capacity of storage media
EF	CO_2e emission conversion factor
EL	economic lifetime of units
$\overline{ELF}$	maximum equivalent loss factor
G^{ing}	solar irradiation forecast
G^{stc}	solar irradiation at standard test condition
i	discount rate
$I^{Net,e}$	binary islanding parameter (1 if grid-connected, 0 if islanded)
$M(\varepsilon)$	required resource for launching a successful attack against a vulnerable unit
N	total number
P^{cap}	allowable power capacity of distributed energy resources
$\overline{P^{Net,e/g}}$	flow limit between the microgrid and the electric/natural gas utility network
pp	normalized generation forecast of non-dispatchable units
Tc, Tr	cell and forecast air temperatures
Thr	storage throughput
v	wind speed forecast
$v^{ci/co/r}$	cut-in, cut-out, and rated speed of wind turbine
α^{ef}	efficiency of units
α^{loss}	energy loss coefficient of storage devices
α^{main}	maintenance coefficient of units
π^{em}	CO_2e tax price
π^{ens}	value of lost load (VOLL)
$\pi^{Net,e}$	electricity purchase/sale price
$\pi^{Net,g}$	natural gas price
π^{peak}	peak demand price
κ	maximum power temperature coefficient
φ	ratio of critical loads to total loads
ψ	disruption cost factor
μ, η	number of days/months per season
ω	present-worth value factor

Variables

E	energy content of storage devices
$E^{\max}$	installed energy capacity of storage devices
EC	microgrid emission cost
ELF	equivalent loss factor
I^{attack}	binary variable indicating cyber-physical attack event (1 if a unit is attacked and consequently disrupted, 0 otherwise)
I^{enc}	reinforcement states of units (1 if reinforced, 0 otherwise)
I^{inv}	investment state of units (1 if installed, 0 otherwise)
IC	microgrid investment cost of units
MC	microgrid maintenance cost
OC	microgrid operation cost/profit
OF	objective function
OF^{attack}	objective function under cyber-attacks
OF^{normal}	objective function under normal conditions
P	output power of distributed energy resources
$P^{dch/ch}$	energy storage discharging/charging power
$P^{ens,l}$	load curtailment for carriers $l \in \{e,t\}$
P^{hyd}	available hydrogen
$P^{\max}$	installed power capacity of distributed energy resources
$P^{Net,e/g}$	exchanged power with the electric/natural gas utility network
$Pref^{hyd}$	anaerobic reactor-reformer system output
PC	microgrid peak demand cost
PD	input electric energy of units comprising {electric heat pump and electrolyzer}
RC	replacement cost of microgrid components
RI	resilience index
Thr^{annual}	annual value of storage throughput
TIC	total investment cost of the project
UC	microgrid's unserved energy cost
$\Re\mathbb{C}$	microgrid's reinforcement cost of units
υ	natural gas consumption by gas-fired units

Specifically, it employs artificial neural networks to forecast the energy consumption of the community. The efficient planning and designing of provisional MGs, as a new class of MGs, is explored in Khodaei (2017) to guarantee the cost-optimal integration of renewable energy resources (RERs), whilst providing economic and environmental benefits for local consumers and wider stakeholders. The financial viability of a campus MG incorporating pre- and post-tax cash flows is investigated in Husein and Chung (2018). The model employs investment-based financial incentives to increase renewable energy penetrations and improve the financial attractiveness of low-emission MGs. A reliable, affordable, clean solution for rural electrification of a village is provided in Kumar et al, (2019) by optimally sizing the RERs in the candidate pool. The model in Kumar et al. (2019) seeks to minimize the levelized cost of energy of the MG reduces by using the demand shifting strategy of

non-essential loads and RER penetrations. A comprehensive battery sizing model for MG applications is proposed in Alsaidan, Khodaei and Gao (2018), which determines the optimal energy and power ratings, technology, and maximum depth of discharge of the battery. The battery lifetime is reflected in the model by means of degradation, which is influenced by the depth of discharge and lifecycle of the battery. A methodology for the optimal sizing of an MG is presented in Prathapaneni and Detroja (2019), which accounts for the lifetime of battery and generator units under a load-following strategy. The model also treats electric vehicles and pumped water storage as dynamic loads, which participate in associated demand response programs. A model is proposed in Nejabatkhah (2018) to optimally size and site photovoltaic (PV) and battery units integrated into an isolated community MG. The model also evaluates the impact of selected units on power quality and system loss. A generic storage sizing methodology is provided in Jacob, Banerjee and Ghosh (2018) to determine the technically feasible and economically viable mixtures of short, medium, and long-term storage units within an islanded solar PV-driven MG. The model's objective is to minimize the annualized life cycle cost of an MG tailored to a remote village comprised of 20 households. Owing to the prohibitive investment cost of distributed energy resources (DERs), a regulated third-party based MG planning approach is presented in Meena, Yang and Zacharis (2019) to alleviate economic barriers in the proliferation of prosumers by luring a larger number of stakeholders to invest in community energy systems via long-term contracts. The associated numerical simulation results indicate that not only does the proposed business model minimize the operational cost of the community, but it is also able to maximize the return on investment. A planning tool is developed in Stevanoni, De Greve, Vallee and Deblecker (2019), which enables prior feasibility analysis of industrial MG developments incorporating multiple stakeholders. The model employs a game-theoretic framework that allows studying different and potentially conflicting objectives of stakeholders. The optimization of maritime port MGs is explored in Molavi, Shi, Wu and Lim (2020) considering model-inherent uncertainties associated with RERs and power outages. The results indicate that port MGs with multiple stakeholders can provide various benefits, such as avoiding critical facility downtime, energy savings, energy self-sufficiency, and emission reduction. A modeling framework for partitioning smart distribution systems into supply-sufficient MGs is proposed (Barani et al., 2019), which focuses on the optimal allocating DERs and reclosers. The paper in Gazijahani and Salehi (2017) proposes an innovative bi-level model for the risk-based optimal design of MGs under uncertainties in demand and renewable generation. The model determines the optimal siting and sizing of DERs together with partitioning the traditional distribution grid into a number of MGs considering the optimal allocation of section switches. Moreover, the optimal techno-economic and capacity optimization of an isolated multi-carrier microgrid (MCMG) is explored in Lorestani, Gharehpetian and Nazari (2019) considering battery degradation and reliability indices. The application of the model to a test-case system highlights the large values of dissipated energy to avoid battery overcharging, which indicates the necessity of more advanced energy planning methods.

The integration of different energy assets tailored to electricity, heat, and natural gas vectors offers a significant diversity necessary for unlocking transformational synergies between substantial increases in the use of electricity and renewable power generation (Guelpa, Bischi, Verda, Chertkov & Lund, 2019). In this context, the term MCMG, which refers to a low- or medium-voltage electrical network hybridized with other energy carrier networks, is clearly defined in Amir, Jadid and Ehsan, (2017), 2019; Azimian, Amir and Haddadipour (2020a). Accordingly, a growing body of literature has formulated a range of solution algorithms for the optimal planning of MCMGs. For instance, an approach for the security-constrained design of an isolated MCMG is proposed in Mashayekh et al. (2018), which ensures the reliability of supply by determining the optimal generation mix, size, and location, whilst adhering to a pre-set power reserve constraint. A multi-stakeholder, multi-agent system is developed in Mohseni and Moghaddas-Tafreshi (2018), which specifically focuses on the modeling of cooperative self-sustainable MCMGs. More specifically, the multi-agent system is comprised of a design agent, a control agent, a generation agent, a load agent, and a charging/refilling station agent. A planning framework is developed in Ma et al. (2018) to design multi-energy systems with the aim of improving the overall economic and environmental efficiencies. Also, a general framework is presented in Olsen, Zhang, Kang, Ortega-Vazquez and Kirschen (2018) to deploy low-carbon multi-energy districts by incentivizing renewable investment. A co-optimization scheme is presented in Yuan, Illindala and Khalsa (2017) to aid the community MG deployments by satisfying the requirements of the U.S. Department of Energy and relevant state renewable energy mandates, whilst additionally providing a platform to measure the impact of regulatory constraints on the pace of MG developments. An MCMG planning method is presented in Cheng, Zhang, Kirschen, Huang and Kang (2020), which accounts for carbon emission reduction targets, and assists the associated decision-making for the development of low-carbon regions with high penetrations of RERs. A scenario-based planning model is introduced in Ehsan and Yang (2019) that provides an efficient solution for the realization of low-cost and low-carbon MCMGs. The model is aware of the problem-inherent uncertainties, such as the uncertainties in the forecasts of renewable generations and multi-energy demands. A multi-period joint expansion planning approach is proposed in Wei, Zhang, Wang, Cao and Khan (2020) to determine the optimal mix, size, and installation time of a diverse set of DERs in MCMG applications. The proposed framework considers both short- and long-term uncertainties of renewable generations, demands, as well as declining trends of battery capital costs. In another instance, the optimal planning of a multi-energy system is carried out in Mansouri, Ahmarinejad, Ansarian, Javadi and Catalao (2020) using a decomposition approach, whilst factoring in the effects of uncertainties in multi-energy demands and wind generation. Moreover, the model exploits the demand shifting potential of customers and explores its impact on the planning solution. The optimal siting and sizing of DERs integrated into a 5-node multi-energy MG is determined under various uncertainties in Yang, Jiang, Cai, Yang and Liu (2020). The model incorporates tractable linearized ac load flow analysis and heat transfer considerations, in accordance with physical, real-world constraints.

A multi-objective co-optimization approach is presented in Chen et al. (2018) to simultaneously optimize the design and operation of a grid-connected MG. An efficient demand response model is also employed in the model to reduce the total discounted system cost yielded by the optimization model without compromising customer satisfaction. A two-stage planning method considering price-based demand response programs tailored to multi-energy systems is proposed in Pan, Gu, Wu, Lu and Lu (2019). The upper stage is designed to minimize the annual capital and operation costs associated with the DERs in the candidate pool. In the lower stage, an integrated demand response program is implemented, where the shiftable loads of customers are modified in response to the nodal energy price calculated in the upper stage, thereby providing the co-benefits of system cost minimization and energy bill savings. The study in Hamad, Nassar, El-Saadany and Salama (2019) designed an efficient stochastic planning model for standalone hybrid AC/DC MGs with the objective of minimizing the planning costs, which consist mainly of the capital investment and operational costs of the DERs and power electronics devices. A probabilistic dynamic planning method is proposed in Senemar, Rastegar, Dabbaghjamanesh and Hatziargyriou (2019) for residential energy systems with the aim of minimizing the levelized cost of energy over the planning horizon. Controllable electrical and thermal appliances have also been employed in the model to cost-effectively handle the variability in the output of solar PV generation. The authors have gone further in Senemar, Seifi, Rastegar and Parvania (2020) and included the excess solar PV energy curtailment costs in the objective function. The numeric results indicate

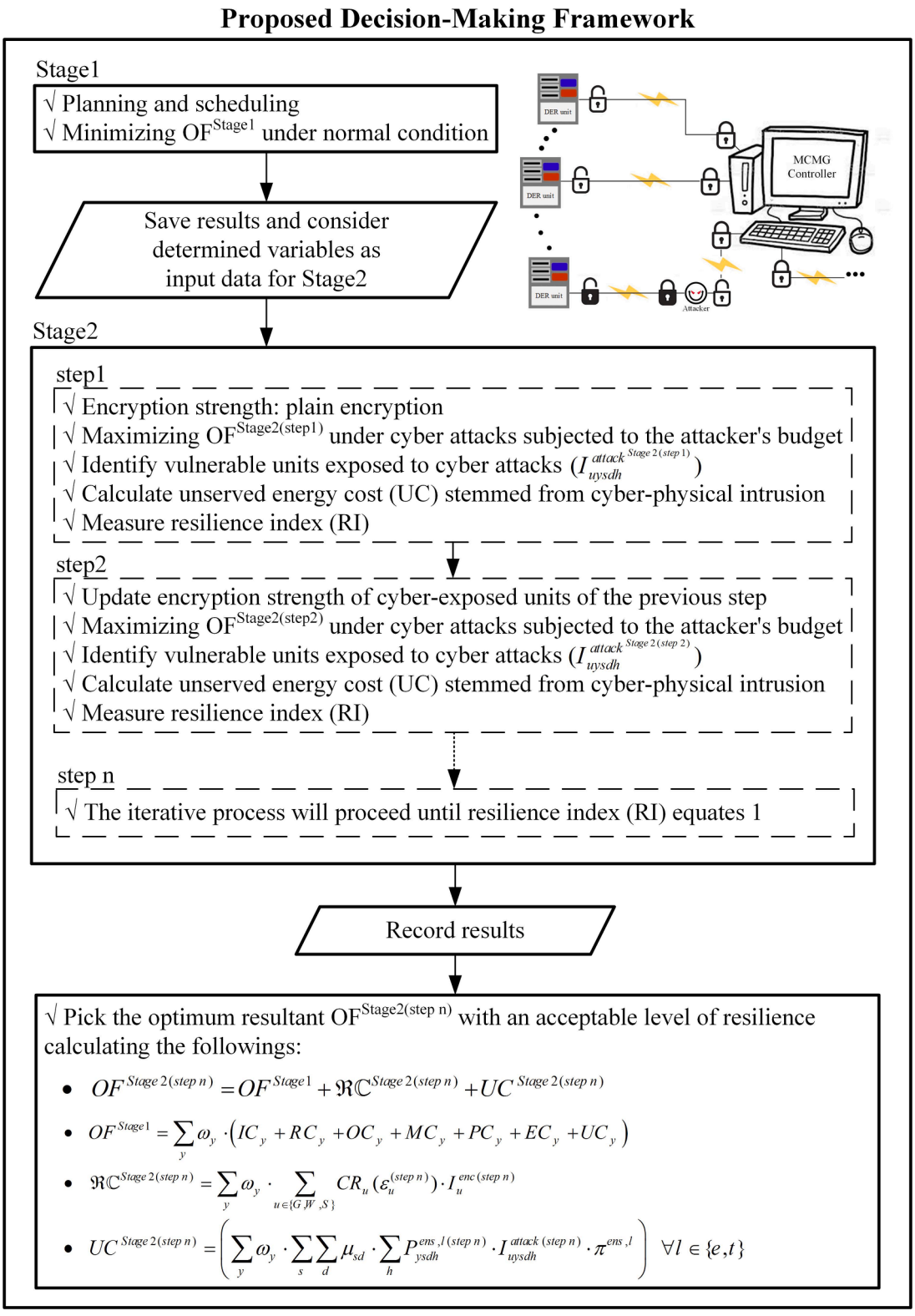

Fig. 1. Flowchart of the Proposed Method for the Resilience Planning of MCMGs under Cyber-Attacks.

the important role of the associated curtailment costs in increasing the penetration of solar PV generation systems in residential community applications. In another instance, a bi-objective model is proposed in Nojavan, Majidi and Esfetanaj (2017) to optimally site and size electrical storage units within a 33-bus MG. The bi-objective model concurrently optimizes the minimization of costs and maximization of the reliability of the MG, whilst additionally implementing a time-of-use demand response program. Similarly, the study in Kiptoo et al. (2019) focuses on the long-term planning of renewables-based MGs with the aim of minimizing life-cycle costs and maximizing reliability, whilst implementing time-based demand response programs – particularly, critical peak pricing – to improve the load factor. Furthermore, the study in Hanna et al. (2019) proposes an optimal MG planning model, which seeks to minimize the capital investment and operational costs, as well

Table 1
Dispatchable and Non-dispatchable Units' Characteristics.

Unit	Allowable installation capacity range (kW)	Capital investment / replacement costs ($/kW)	Maintenance coefficient ($/kWh)	Electrical/thermal efficiency (%)	Availability (%)	Lifetime (year)
CHP	5–15,000	300/300	0.01258	35/50	96	20
FC	10–15,000	1500/1500	0.00900	50/34	100	5
Boiler	4–15,000	45/45	0.00870	0/90	97	10
EHP	4–15,000	250/250	0.00300	97/0	98	15
PV	5–15,000	550/550	0.00310	–	96	25
WT	5–15,000	650/650	0.00600	90/0	96	25

Table 2
Energy Storage Characteristics.

Unit type	Allowable installation capacity range		Capital investment / replacement costs		Efficiency (%)	Loss efficiency (%)	Depth of discharge (%)	Throughput (kWh)	Availability (%)	Lifetime (year)
	Power ($/kW)	Energy ($/kWh)	Power ($/kW)	Energy ($/kWh)						
ESS	1–15,000	1–15,000	30/20	75/37	93	5	80	3000	96	5
TSS	1–15,000	50–15,000	5/5	33/30	90	5	100	–	100	15
HSS	1–15,000	50–15,000	5/5	12/11	98	5	100	–	100	15

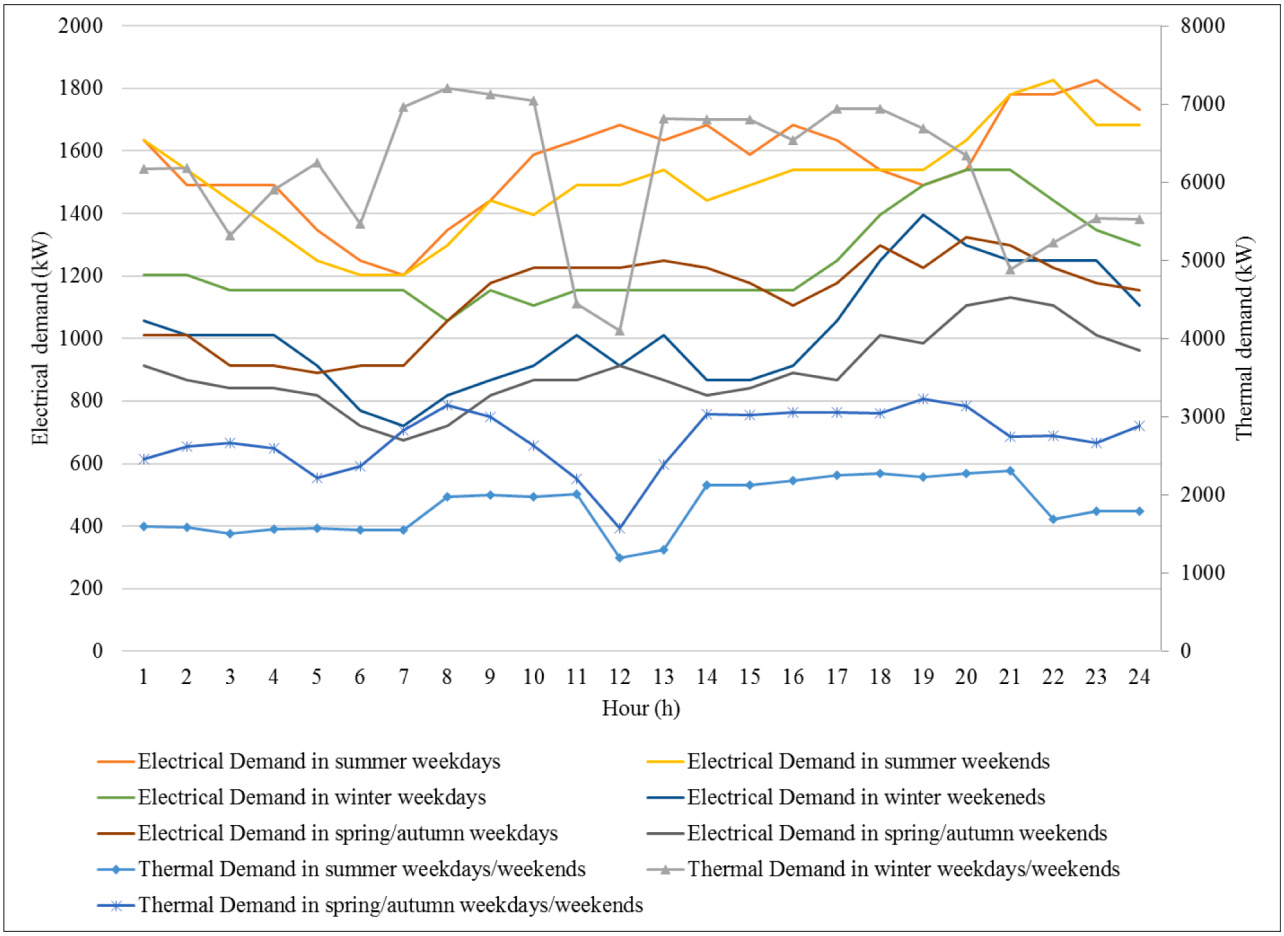

Fig. 2. Average Value of Loads in the First Year.

as the costs of load interruption using a single objective function. It also introduces the notion of customer damage as a function of the customer-specific duration of interruption for the valuation of the cost of energy unserved. Based on numeric simulation results, the authors have shown that the proposed method is able to improve the cost-efficiency of a test-case system by up to 4.15%. Moreover, a generic planning model is presented in Adefarati and Bansal (2019) to assist MG planners in exploring the effects of high penetration of RERs on the economic, reliability and environmental trade-offs of bulk power systems. To this end, a specific objective function is developed that incorporates the whole-life energy costs, loss of load costs, and emissions penalties. In addition, a multi-objective optimization framework is presented in Fioriti, Pintus, Lutzemberger and Poli (2020) to optimally design an off-grid rural MG with the aim of minimizing the costs associated with

Table 3
Hourly electricity market price.

Time (h)	1	2	3	4	5	6
Price ($/kWh)	0.090	0.093	0.077	0.074	0.068	0.082
Time (h)	7	8	9	10	11	12
Price ($/kWh)	0.088	0.098	0.097	0.096	0.083	0.081
Time (h)	13	14	15	16	17	18
Price ($/kWh)	0.078	0.073	0.066	0.076	0.106	0.118
Time (h)	19	20	21	22	23	24
Price ($/kWh)	0.102	0.104	0.086	0.073	0.081	0.072

Table 4
MCMG parameters.

Discount rate (%)	5	Value of lost load ($/kWh)	Electricity	3.65
Annual load growth rate (%)	2.9		Heat	0.107
Annual electricity price growth rate (%)	2.5	Emission factor (kg/kWh)	Utility	0.2556
Monthly demand charge ($/kW)	6.192		CHP	0.17606
Equivalent loss factor (%)	0.01		Boiler	0.226
Budget limit of the attacker ($/year)	30,000		Fuel cell	0.287
		CO_2e tax price ($/kg-$CO_2$e)		0.0276

the capital investment, replacement, as well as operation and maintenance of candidate DERs. To verify the effectiveness of the proposed model in designing economically viable stand-alone MGs, the authors conducted capital budgeting analysis based on the modified internal rate of return metric.

The major power outage events and their underlying reasons are reviewed in Hussain, Bui and Kim (2019), where the overall probability of occurrence of a cyber-attack against critical energy infrastructure has been found to be 1.43% based on a comprehensive survey. The most frequent cyber threats have also been found to be a denial of service, corrupted measurements, compromised control commands, load-redistribution attacks, authentication, and buffer overflow (Kaviani & Hedman, 2019; Li, Shahidehpour, Aminifar, Alabdulwahab & Al-Turki, 2017; Li, Shahidehpour & Aminifar, 2017; Manshadi & Khodayar, 2015). In this setting, the strand of the optimal MG sizing literature focused particularly on resilience-oriented frameworks has been reviewed in Wang, Rousis and Strbac, (2020), which highlights the general lack of methods robust to cyber-attacks. For example, an optimization model is developed in Chalil et al. (2018) for the capacity planning and resilient operation of remote MGs subject to N-1 security constraints. In another instance, an efficient market-based, resilience-aware planning framework is developed in Khayatian, Barati and Lim (2018), which facilitates the deployment of MGs in rural electrification applications. In the proposed framework, the owners of the generation system, the transmission network, and the community MG load aggregator are treated as individual, utility-maximizing decision-makers who interact in a specifically developed market. The principal resilience consideration in the proposed model is accounting for the outages of the components. Also, an optimal MG designing framework tailored to battery-assisted, solar PV-driven MGs is provided in Rosales-Asensio, de Simón-Martín, Borge-Diez, Blanes-Peiró and Colmenar-Santos (2019), which factors in the battery bank autonomy and grid outage survivability as resilience metrics. Based on numeric simulations, it has been shown that the proposed model is able to provide up to 4 h of autonomy, with a blackout survival probability of 40%. Furthermore, an MG capacity planning optimization framework is presented in Chen et al. (2020), which characterizes the uncertainty associated with power

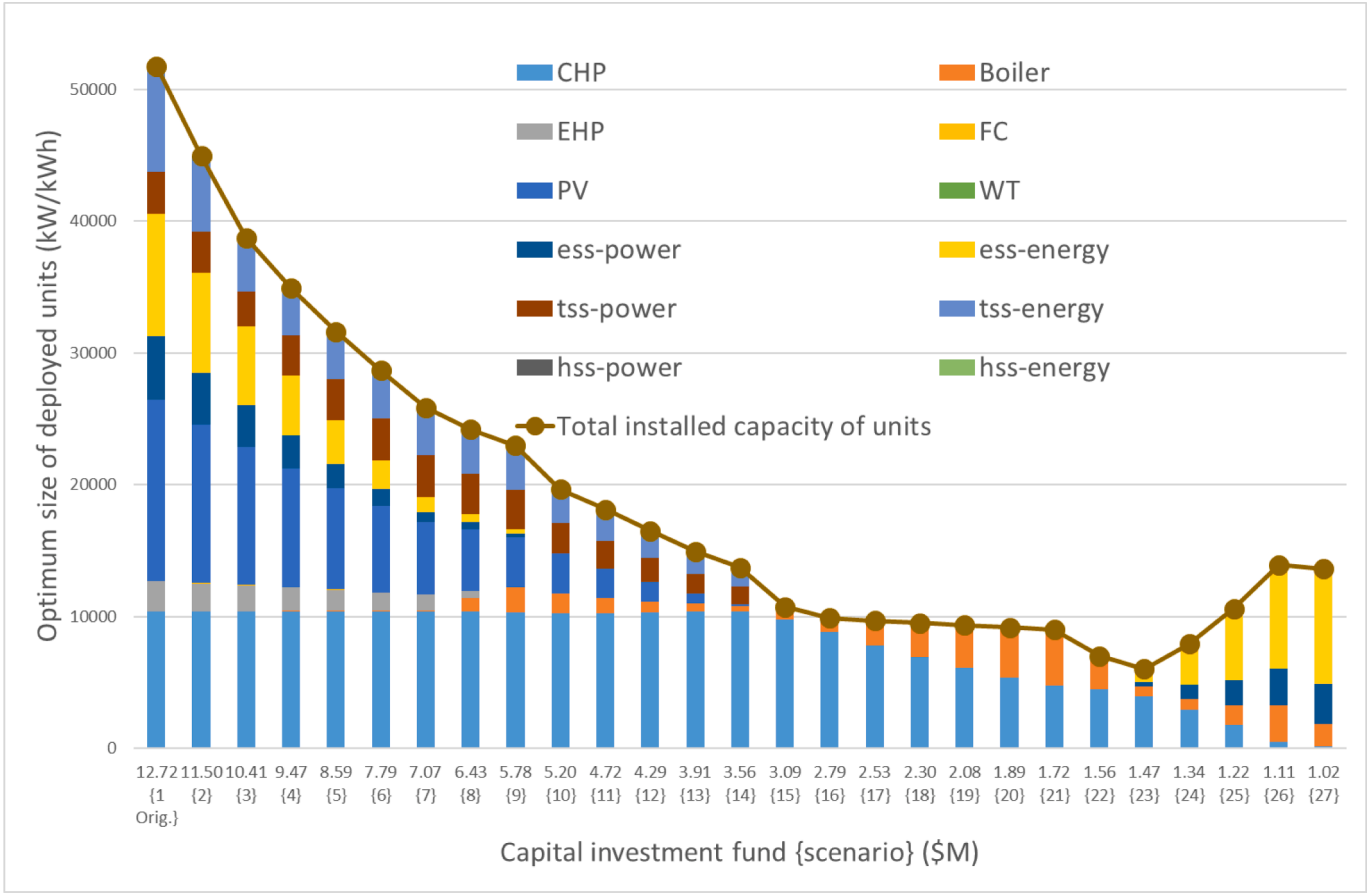

Fig. 3. Optimum Size of Candidate MCMG Technologies as a Function of CIF.

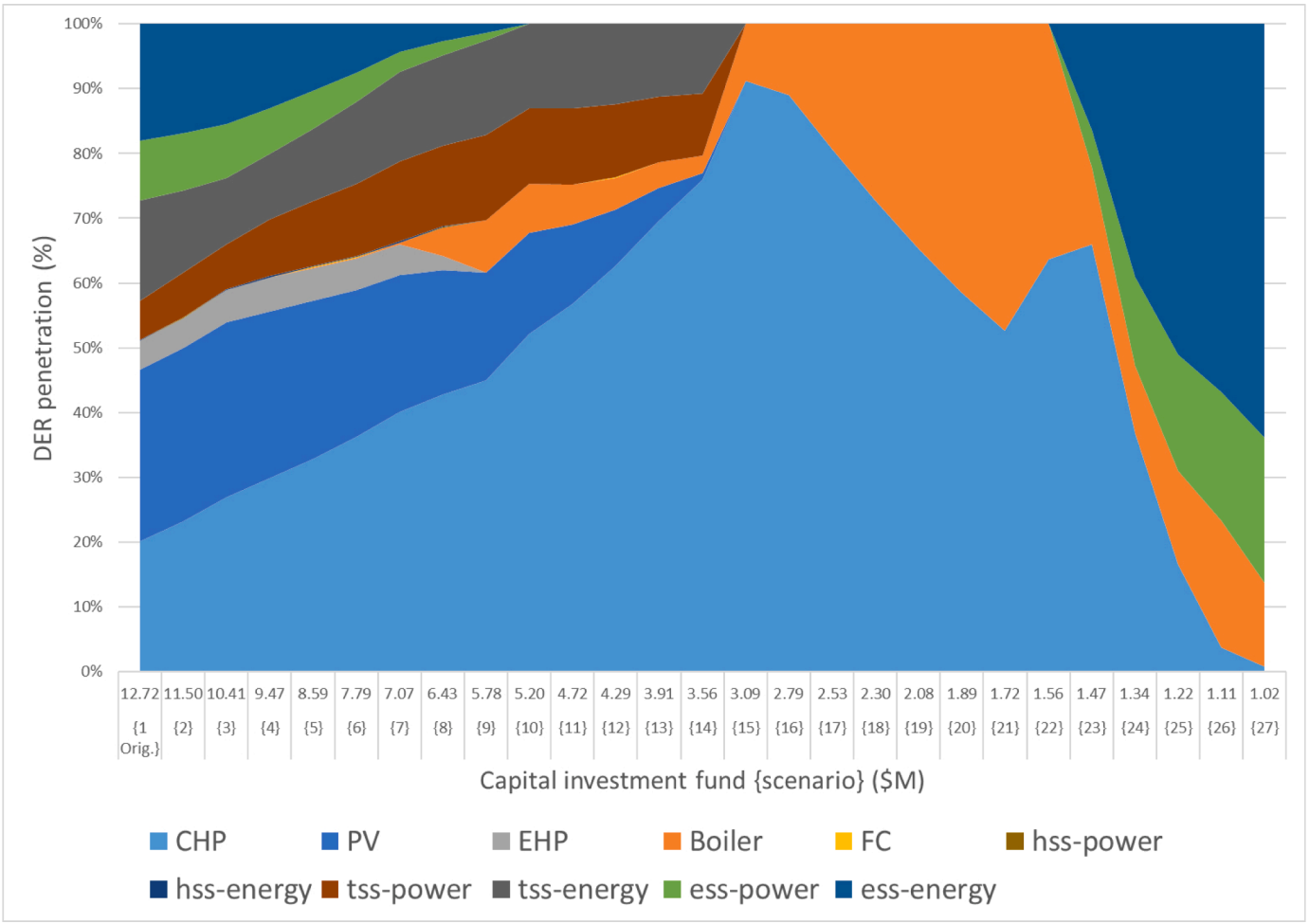

Fig. 4. Optimized Units' Penetration as a Function of CIF.

line failure and renewable generation outage, towards maximizing the resilience of the system in serving the critical loads against such system disruptions. Moreover, a resilience-focused MG planning model is presented in Wu et al. (2019) to coordinately determine the optimal capacity of candidate DERs and distribution lines, whilst ensuring a pre-specified level of resilience against system-wide contingencies. To this end, a specifically formulated loss of load constraint is used to quantify the resilience of the MG against contingencies. Also, the optimal size of DERs integrated into a military-based MG, whilst meeting a pre-defined resilience goal against extended outages is addressed in Wu, Ma, Huang, Fu and Balducci (2020). The model additionally quantifies the uncertainty in loads, renewable generation, and operational grid disturbances. Furthermore, the resilience of an overall distribution system, which consists of networked MGs, could be strengthened by simultaneously accounting for line hardening and added infrastructure options in the optimal planning model (Barnes, Nagarajan, Yamangil, Bent & Backhaus, 2019). Interestingly, the numeric simulation results indicate that networked MGs are able to entirely eliminate the need for line hardening and added infrastructure options for the supply of critical loads compared to the baseline case of a centralized radial distribution network. Similarly, the study in Xie, Teng, Xu and Wang (2019) has also focused on the resilient designing of networked MGs by comparing the efficiency of various battery operation strategies. In contrast to the study in Barnes et al. (2019), the numeric results indicate that the reliable and robust supply of critical loads under extreme fault conditions requires the allocation of additional battery capacity to the networked MGs. In the same vein, the study in Pecenak, Stadler, Mathiesen, Fahy and Kleissl (2020) proposes a novel hybrid optimization framework to design resilience-oriented MGs that use added battery storage capacity – with specific charge/discharge rate optimization – to effectively hedge against extended grid outages.

As the above comprehensive review of the mainstream literature indicates, the resilient designing of MCMGs under cyber-attacks has not yet been addressed. In response, this paper introduces a novel MCMG planning optimization model that is aware of the pre-defined levels of resilience against low-probability high-impact events. The proposed MCMG planning model is used to optimally serve the energy requirements of a group of industrial customers using various DERs, namely combined heat and power (CHP) units, natural gas boilers, electric heat pumps (EHPs), renewable energy technologies, fuel cells (FCs), and storage units. Not only is the model able to determine the optimal mix and size of candidate DERs for integration into the MCMG, but it also, more importantly, reinforces the key components needed to serve the critical loads in circumstances of active cyber-attacks – including intentional attempts to affect the operation of the system. The main objective of the model is to minimize the total planning cost, incorporating the capital investment, replacement, as well as operation and maintenance costs of candidate DERs, potential peak demand charges, emissions penalties, costs of unserved energy, and necessary reinforcement cost of the MCMG, subject to a pre-specified robustness level against unplanned, cyber-attack-induced grid outages. To alleviate the computational burden, two typical days of summer, winter, and the transitional spring/autumn seasons are selected to represent the year-long operation of the system. The problem is formulated as a mixed-integer programming problem and solved using the GAMS 24.1 software. Furthermore, a novel index is presented, for the first time in the

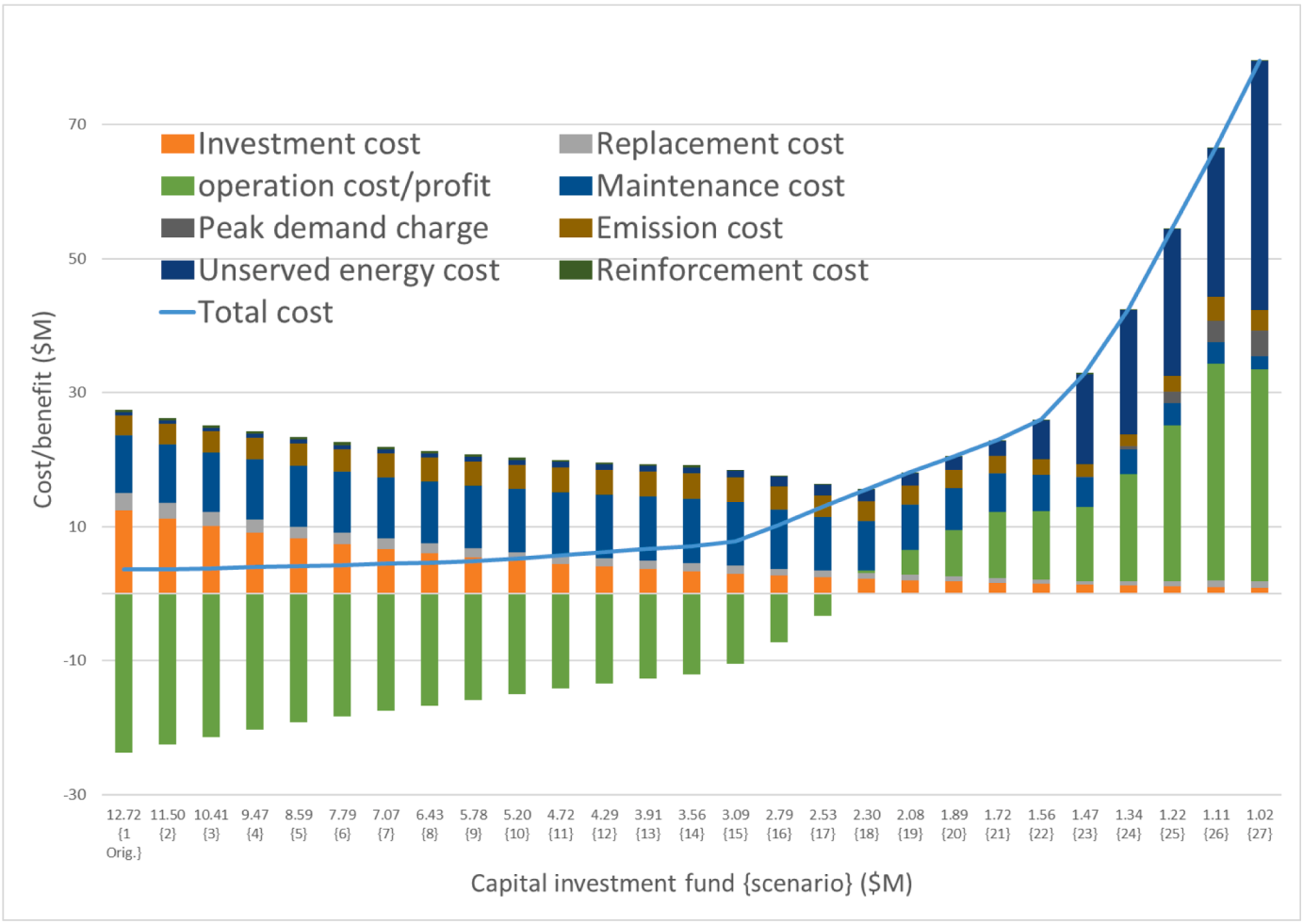

Fig. 5. Total Cost Breakdown of the MCMG as a Function of the CIF.

literature, to quantify the resilience of MCMGs against intentional grid and infrastructure disruptions. More specifically, the key contributions of the paper are:

- Determining the cost-optimal mix and size of DERs for integration into MCMGs considering reliability and environmental constraints.
- Calculating the size of the added infrastructure needed to tolerate the cyber-physical attacks by serving the critical loads and quantifying the impact on the total MCMG development costs.
- Applying preventive reinforcement strategies to ensure the resilient design and operation of the proposed MCMG against cyber-physical attacks.
- Quantifying the additional capital investment requirements in light of increased resilience, as well as the associated changes in the optimal size and economic viability of MCMGs – using various financial appraisal metrics, such as present-worth value, levelized cost of energy, discounted payback period, and profitability index.
- Assisting the associated decision-making processes in deploying cyber-attack-resilient MCMGs.

On a wider level, the proposed model provides a platform to produce a set of case-specific preventive actions and infrastructure capacity reinforcement decisions for the resilient operation of MCMGs, with a particular focus on meeting the critical loads, which otherwise remain unmet during the associated restoration times. More specifically, the model (i) enables seamless islanding by installing additional dispatchable DERs for an uninterrupted supply of critical loads during disturbances, particularly cyber-attacks, (ii) employs a specifically developed reliability index to constrain the total annual curtailed electrical loads, (iii) utilizes a specifically developed resilience index to quantify the system's vulnerability to contingencies precipitated by intentional cyber disruptions and reinforce the system to the designer's desired level, and (iv) paves the way for the incorporation of advanced encryption techniques for fast control systems that maintain the overall system stability – and provide an effective hedge against cyber-physical attacks to MGs.

The remainder of this paper is organized as follows. Sections 2 formulates the proposed resilience-oriented MCMG planning modeling framework. Section 3 conducts numerical simulations on a test-case MCMG and discusses the results. Finally, conclusions are drawn in Section 4, whilst also highlighting the evidence-based real-world advantages of using the proposed method.

2. Methodology

This section mathematically formulates the proposed method for the resilient development of MCMGs subject to cyber-attacks – which lead to physical unit disruptions. The cyber-resilient MG planning in this paper is performed under a set of assumptions, namely:

(1) The attacker seeks to increase the frequency and duration of service interruptions by disrupting the MG's physical units by coordinated, remote, cyber intrusions. A cyber-physical attack against critical infrastructure occurs when a hacker gains access to the encrypted data packets received by the physical unit

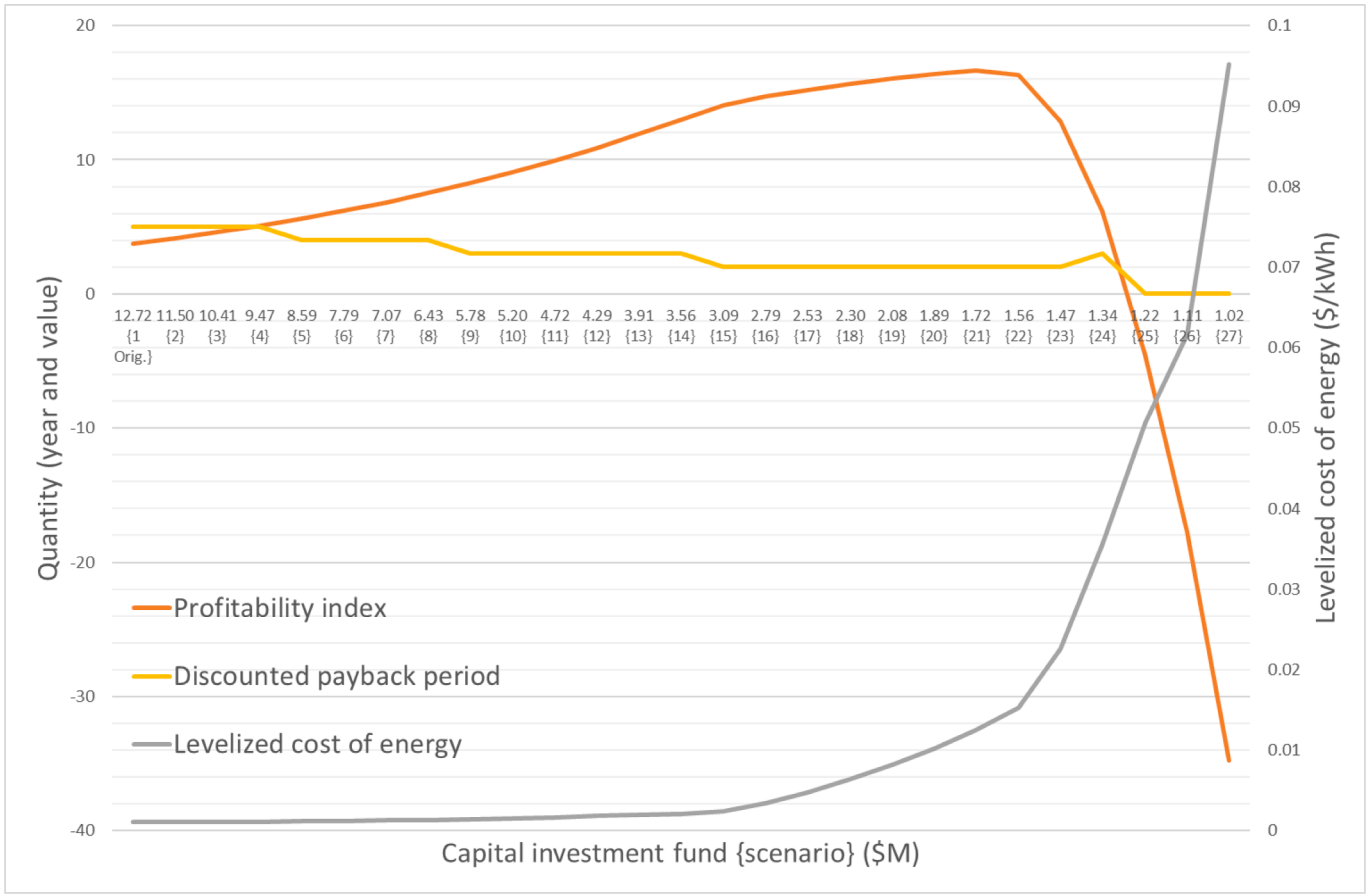

Fig. 6. Capital Budgeting Analysis of the Proposed MCMG with Respect to CIF Variations.

controller, and then decrypts and manipulates the control signals sent from the MCMG's central controller to the underlying assets.

(2) For practical reasons, it is assumed that the attacker might only gain unauthorised access to the breakers connecting the associated units to the MCMG's common bus, and subsequently open the relevant breakers. This consequently disables the MCMG operator's remote access to the associated components. The interested reader is referred to (Venkataramanan et al., 2019) for the detailed steps undertaken for generating a set of hypothetical random cyber-attacks, which are inspired by a recent cyber-attack in Ukraine. Also, the encryption techniques developed in Barnes et al. (2019); ISO-NE (2015) are used in the proposed model to reinforce the most vulnerable and influential units against cyber-attacks.

(3) An encryption code for the data packets broadcasted to each of the MCMG's physical units is assumed to be present. The encryption key disallows intruders to read, intercept, or manipulate the control signals. Expectedly, the greater the encryption strength, the higher the associated costs of both encryption and decryptions, thereby offering better protection during a cyber-attack on the MCMG's infrastructure.

Mathematically, the proposed cyber-resilient MCMG deployment is formulated as a two-stage optimization problem. In the first stage, the optimal mix and size of the candidate units over the planning horizon are determined subject to unplanned grid outages. In the second stage, the preventive reinforcement strategy is implemented by identifying and planning for the cyber-attack-prone units. An iterative approach is used in the second stage to tailor the solution to the developer's desired level of resilience. The iterative approach gradually increases the robustness of the MCMG design based on preventive reinforcement schemes. Put differently, the second stage seeks to increase the encryption strength of the vulnerable physical units using an iterative optimization approach that identifies and reinforces the vulnerable physical units based on the maximum possible MCMG operating cost during attacks (representing the worst-case scenario), in accordance with pre-specified attacker budgets to trigger disruptions.

Accordingly, the overall model, expressed in Eq. (1), minimizes the MCMG's total investment planning cost, which incorporates the investment, replacement, as well as operation and maintenance costs of DERs, potential peak demand charges, emission costs, unserved energy costs, and the associated reinforcement costs. The investment cost of DERs (Eq. (2)) represents the capital cost of dispatchable and non-dispatchable distributed generators (DGs) – derived by multiplying the DGs' capital costs by the corresponding optimized power capacities – as well as the capital cost of storage systems, in accordance with the corresponding optimized power and energy capacities – calculated by multiplying the storage systems' capital costs by the corresponding optimized power and energy capacities. The replacement cost of DERs is calculated using Eq. (3) as a function of the number of replacements over the planning horizon and the associated installed power/energy capacities. The operation cost in Eq. (4) determines the net cost of exchanged power with the wider electric and natural gas utility networks. The operation and maintenance costs of the selected dispatchable and non-dispatchable units are given in Eq. (5), which are functions of the optimal capacities of the units multiplied by the associated maintenance coefficients. Demand charges are applied to large-scale commercial and industrial based on the maximum amount of power that a customer used in any interval. The demand charge is calculated in Eq. (6), where the demand charge rate is multiplied by the maximum amount of electricity imported from the utility grid. Note that the plus sign in the superscript of the variable representing the power exchanges with the wider

Table 5
Iteration-Wise Comparative Results of the Preventive Reinforcement Process for Various CIF Values.

CIF ($m)	Iter.	RI	Plan. cost ($m)	Reinf. cost ($m)	Total cost ($m)	Disrupted units
12.72	1	0.20634	4.46	0.09	4.56	CHP, PV
{1}	2	0.49275	3.81	0.12	3.93	CHP, PV, ESS
	3	0.82888	3.42	0.19	3.61	ESS, TSS
	4	0.98773	3.29	0.23	**3.51**	EHP, TSS
	5	0.99499	3.283	0.27	3.55	EHP, FC
	6	0.99927	3.2801	0.30	3.59	FC
	7	1	3.2796	0.33	3.61	
9.47	1	0.20735	4.75	0.11	4.85	CHP
{4}	2	0.38504	4.28	0.12	4.40	PV
	3	0.53031	4.04	0.13	4.17	CHP, ESS
	4	0.71654	3.82	0.17	3.99	PV, TSS
	5	0.89296	3.65	0.21	3.86	EHP, ESS
	6	0.99283	3.571	0.25	**3.82**	FC, TSS
	7	0.99655	3.568	0.29	3.86	Boiler, EHP
	8	0.99927	3.566	0.33	3.90	FC
	9	0.99999	3.5653	0.36	3.92	Boiler
	10	1	3.5652	0.38	3.95	
7.79	1	0.20895	5.07	0.11	5.18	CHP
{6}	2	0.46737	4.47	0.12	4.59	CHP, PV
	3	0.74146	4.12	0.16	4.28	PV, ESS
	4	0.93355	3.95	0.20	4.15	ESS, TSS
	5	0.99106	3.91	0.24	**4.14**	EHP, FC, TSS
	6	0.99762	3.901	0.29	4.19	Boiler, EHP, FC
	7	0.99997	3.899	0.36	4.26	Boiler
	8	1	3.899	0.38	4.28	
6.43	1	0.21030	5.45	0.11	5.56	CHP
{8}	2	0.50212	4.80	0.12	4.92	CHP, PV
	3	0.82290	4.43	0.16	4.59	PV, ESS
	4	0.96738	4.31	0.20	**4.50**	ESS, TSS
	5	0.99245	4.29	0.24	4.53	Boiler, EHP, FC, TSS
	6	0.99864	4.282	0.30	4.59	Boiler, EHP, FC
	7	1	4.281	0.38	4.67	
5.20	1	0.21402	6.10	0.07	6.16	CHP
{10}	2	0.53426	5.41	0.08	5.49	CHP, PV
	3	0.89056	5.03	0.12	5.15	PV, TSS
	4	0.99292	4.95	0.16	**5.11**	Boiler, FC, TSS
	5	0.99816	4.943	0.21	5.15	Boiler, FC
	6	1	4.941	0.27	5.21	
3.09	1	0.22733	8.87	0.03	8.90	CHP
{15}	2	0.60981	8.13	0.04	8.17	CHP, Boiler
	3	0.99917	7.762	0.08	**7.84**	Boiler
	4	1	7.761	0.11	7.87	
1.47	1	0.54860	33.24	0.04	33.28	CHP
{23}	2	0.79935	32.95	0.05	33.01	CHP, ESS
	3	0.97502	32.81	0.09	**32.90**	Boiler, ESS
	4	0.99852	32.787	0.13	32.92	Boiler
	5	1	32.786	0.16	32.95	
1.02	1	0.56717	79.85	0.04	79.89	ESS
{27}	2	0.81385	79.58	0.05	79.63	CHP, ESS
	3	0.98925	79.429	0.09	**79.52**	Boiler
	4	0.99426	79.425	0.11	79.53	CHP
	5	0.99640	79.423	0.13	79.56	Boiler
	6	1	79.421	0.16	79.58	

Key: CIF = Capital investment fund, Iter. = Iteration, RI = Resilience index, Plan. = Planning, Reinf. = Reinforcement.

electrical network (denoted by $P^{Net,e,+}_{ysdh}$) indicates that the peak demand charge is specifically applied to the maximum positive value of net imports (imports minus exports) to ensure that exports are not linked to such peak demand charges. Also, in Eq. (6), μ_{sd} and η_s denote the number of days per season and the number of months per season, respectively. The emissions cost of the utility grid and non-renewable DGs is calculated in Eq. (7). Eq. (8) represents the cost of unserved electrical and thermal demands, which is defined as the amount of load curtailments multiplied by the value of lost loads (VOLLs). The annual reinforcement cost is expressed in Eq. (9), which denotes the capital cost of reinforced DERs (as a function of the physical unit's encryption strength) multiplied by their reinforcement states. It is noteworthy that DER investment and encryption costs are incurred at the beginning of the first year. Furthermore, Eq. (10) expresses the present-worth value factor.

$$OF = \sum_{y} \omega_y \cdot \left(IC_y + RC_y + OC_y + MC_y + PC_y + EC_y + UC_y + \Re\mathbb{C}_y\right) \tag{1}$$

$$IC_y = \sum_{u\in\{G,W\}} CC_u \cdot P^{\max}_u + \sum_{u\in S}\left(CP_u \cdot P^{\max}_u + CE_u \cdot E^{\max}_u\right) \qquad \forall y = 1 \tag{2}$$

$$RC_y = \sum_{u\in\{G,W\}} CCr_u\left(r_{uy}\right) \cdot P^{\max}_u + \sum_{u\in S}\left(CPr_u\left(r_{uy}\right) \cdot P^{\max}_u + CEr_u\left(r_{uy}\right) \cdot E^{\max}_u\right) \tag{3}$$

$$OC_y = \sum_{s}\sum_{d} \mu_{sd} \cdot \sum_{h}\left(P^{Net,e}_{ysdh} \cdot \pi^{Net,e}_{yh} + P^{Net,g}_{ysdh} \cdot \pi^{Net,g}_{y}\right) \tag{4}$$

$$MC_y = \sum_{s}\sum_{d} \mu_{sd} \cdot \sum_{h}\sum_{u\in\{G,W\}} P_{uysdh} \cdot \alpha^{main}_u \tag{5}$$

$$PC_y = \sum_{s} \eta_s \cdot \pi^{peak} \cdot \max\left(P^{Net,e,+}_{ysdh}\right) \tag{6}$$

$$EC_y = \sum_{s}\sum_{d} \mu_{sd} \cdot \sum_{h} \pi^{em} \cdot \left(P^{Net,e}_{ysdh} \cdot EF^{Net,e} + \sum_{u\in\{G,W\}} P_{uysdh} \cdot EF_u\right) \tag{7}$$

$$UC_y = \sum_{s}\sum_{d} \mu_{sd} \cdot \sum_{h} P^{ens,l}_{ysdh} \cdot \pi^{ens,l} \qquad \forall l \in \{e,t\} \tag{8}$$

$$\Re\mathbb{C}_y = \sum_{u\in\{G,W,S\}} CR_u(\varepsilon_u) \cdot I^{enc}_u \tag{9}$$

$$\omega_y = 1/(1+i)^{y-1} \tag{10}$$

The objective function is also subject to a set of operational-, investment-level constraints expressed in Eqs. (11)–(37).

2.1. Power balance constraints

Eq. (11) ensures the system-wide power balance by enforcing the sum of power outputs from DERs, the net electricity imports from the utility grid, and the unmet electricity demand to be equal to the sum of the original electrical demand and the energy consumed by the EHP and electrolyzer units. Similarly, the thermal demand balance constraint of the system is expressed in Eq. (12), which ensures that the sum of the thermal energy generations of DERs and the curtailed thermal demand is greater than or equal to the original thermal demand of the customers. Also, the total natural gas consumption of the CHP and gas boiler units is presented in Eq. (13). Furthermore, the FC uses the hydrogen generated by the reactor-reformer system, the hydrogen storage system (HSS), and the electrolyzer unit stored in the dedicated tank, as expressed in Eq. (14). It is assumed that the reactor-reformer system uses municipal solid waste as an available energy resource that can be collected from residential, agricultural, and industrial sectors. The amount of hydrogen produced by the reactor-reformer system is a function of the mass of municipal solid waste collected from the site of interest (Mohseni & Moghaddas-Tafreshi, 2018).

$$\sum_{u\in\{G,W\}} P^{e}_{uysdh} \pm \sum_{u\in ess} P^{dch/ch}_{uysdh} + P^{Net,e}_{ysdh} + P^{ens,e}_{ysdh} = D^{e}_{ysdh} + \sum_{u\in\{ehp,electro\}} PD^{e}_{uysdh} \tag{11}$$

$$\sum_{u\in G} P^{t}_{uysdh} \pm \sum_{u\in tss} P^{dch/ch}_{uysdh} + P^{ens,t}_{ysdh} \geq D^{t}_{ysdh} \tag{12}$$

$$P^{Net,g}_{ysdh} = \sum_{u\in\{chp,boiler\}} \upsilon_{uysdh} \tag{13}$$

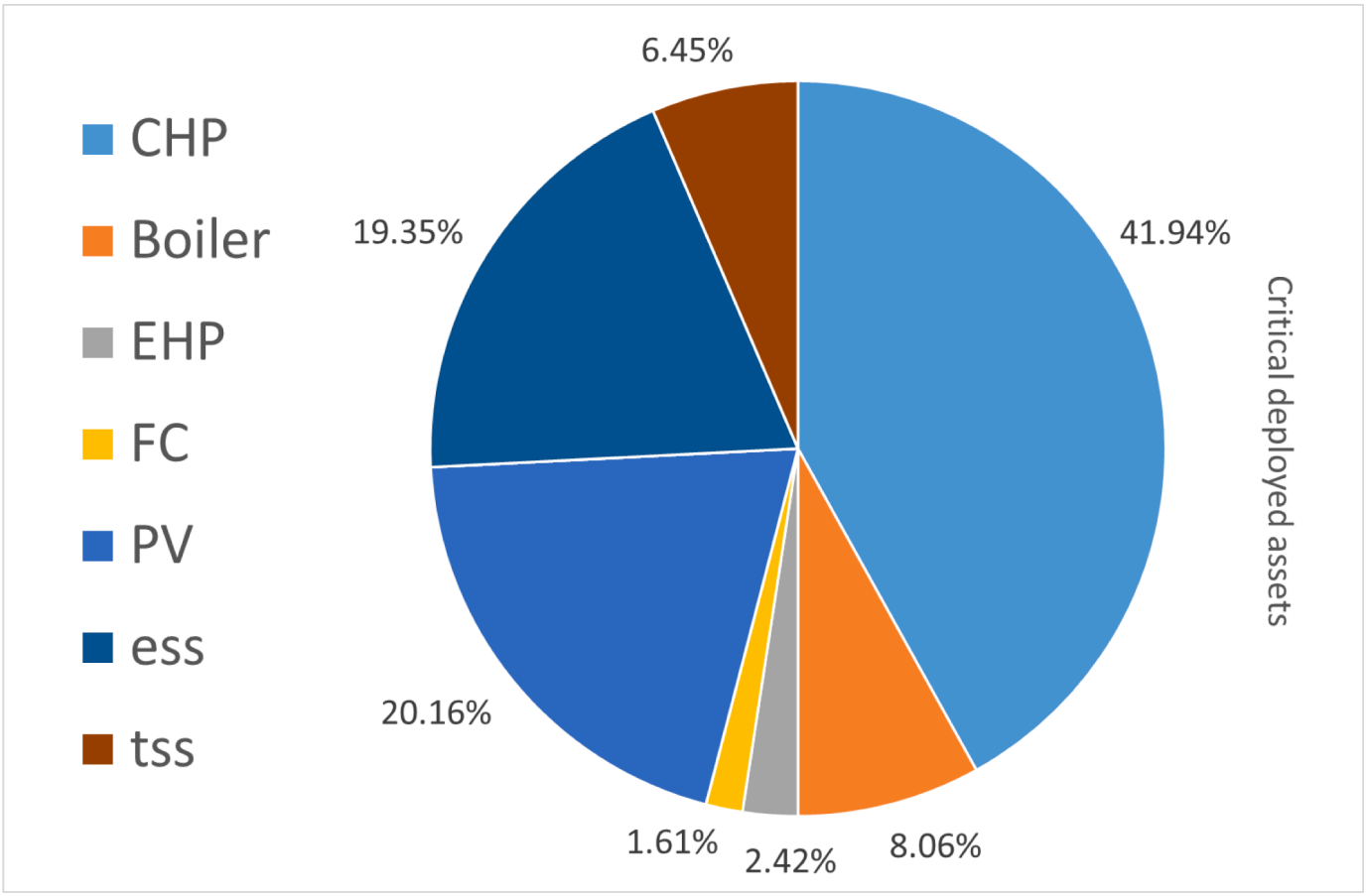

Fig. 7. Percentage Frequency of the Intentional Cyber Disruption of the MCMG's Components.

$$P^{hyd}_{ysdh} = Pref^{hyd}_{uysdh} \pm \sum_{u\in hss} P^{dch/ch}_{uysdh} + \sum_{u\in electro} PD^{e}_{uysdh}\cdot\alpha^{ef}_{u} \tag{14}$$

2.2. Dispatchable and non-dispatchable units' constraints

The energy generation units, including gas-fired units, EHP, FC, PV, and wind turbine (WT) are modeled in Eqs. (15)–(20), respectively. It is noteworthy that the hourly power generation of the PV unit (Eq. (18)) is modeled as a function of solar irradiance and ambient temperature (Azimian, Amir & Javadi, 2020b). In addition, the overall degradation of the PV unit for Yingly Panels over 25 years is accounted for in the model. Similarly, the power curve (Eq. (19)) is used to correspond the WT unit's power output to wind speed forecasts. The hourly generated power by dispatchable and non-dispatchable units is constrained by the corresponding optimum capacities (Eq. (20)). Moreover, the availability or unavailability states of the units under consideration are considered by defining a binary variable that represents the state of the physical units under cyber-attacks; it takes on a value of if the corresponding physical unit is disrupted at a particular time-step (and hence, unavailable), and 0 if it is not disrupted and is available.

$$P^{l}_{uysdh} = v_{uysdh}\cdot\alpha^{ef,l}_{u}\cdot A_{u} \qquad \forall u\in\{chp, boiler\},\ \forall l\in\{e,t\} \tag{15}$$

$$P^{t}_{uysdh} = PD^{e}_{uysdh}\cdot\alpha^{ef}_{ush}\cdot A_{u} \qquad \forall u\in ehp \tag{16}$$

$$P^{l}_{uysdh} = P^{hyd}_{ysdh}\cdot\alpha^{ef,l}_{u}\cdot A_{u} \qquad \forall u\in fc,\ \forall l\in\{e,t\} \tag{17}$$

$$P_{uysdh} = \left(P^{\max}_{u}\cdot\alpha^{ef}_{uy}\cdot A_{u}\cdot\widetilde{pp}_{uh}\cdot\widetilde{G^{ing}_{s}}\cdot(1+\kappa\cdot(Tc-\widetilde{Tr_{s}}))\right)\Big/ G^{stc} \quad \forall u\in pv \tag{18}$$

$$P_{uysdh} = \begin{cases} 0 & 0\le\widetilde{v}_{s}\le v^{ci} \quad or \quad \widetilde{v}_{s}\ge v^{co} \\ P^{\max}_{u}\cdot\alpha^{ef}_{u}\cdot A_{u}\cdot\widetilde{pp}_{uh}\cdot\dfrac{\widetilde{v}^{2}_{s}-v^{ci^2}}{v^{r^2}-v^{ci^2}} & v^{ci}\le\widetilde{v}_{s}\le v^{r} \\ P^{\max}_{u}\cdot\alpha^{ef}_{u}\cdot A_{u}\cdot\widetilde{pp}_{uh} & v^{r}\le\widetilde{v}_{s}\le v^{co} \end{cases} \qquad \forall u\in wt \tag{19}$$

$$0\le P_{uysdh}\le P^{\max}_{u}\cdot\left(1-I^{attack}_{uysdh}\right) \qquad \forall u\in\{G,W\} \tag{20}$$

2.3. Storage systems' constraints

The energy storage-related constraints are presented in Eqs. (21)–

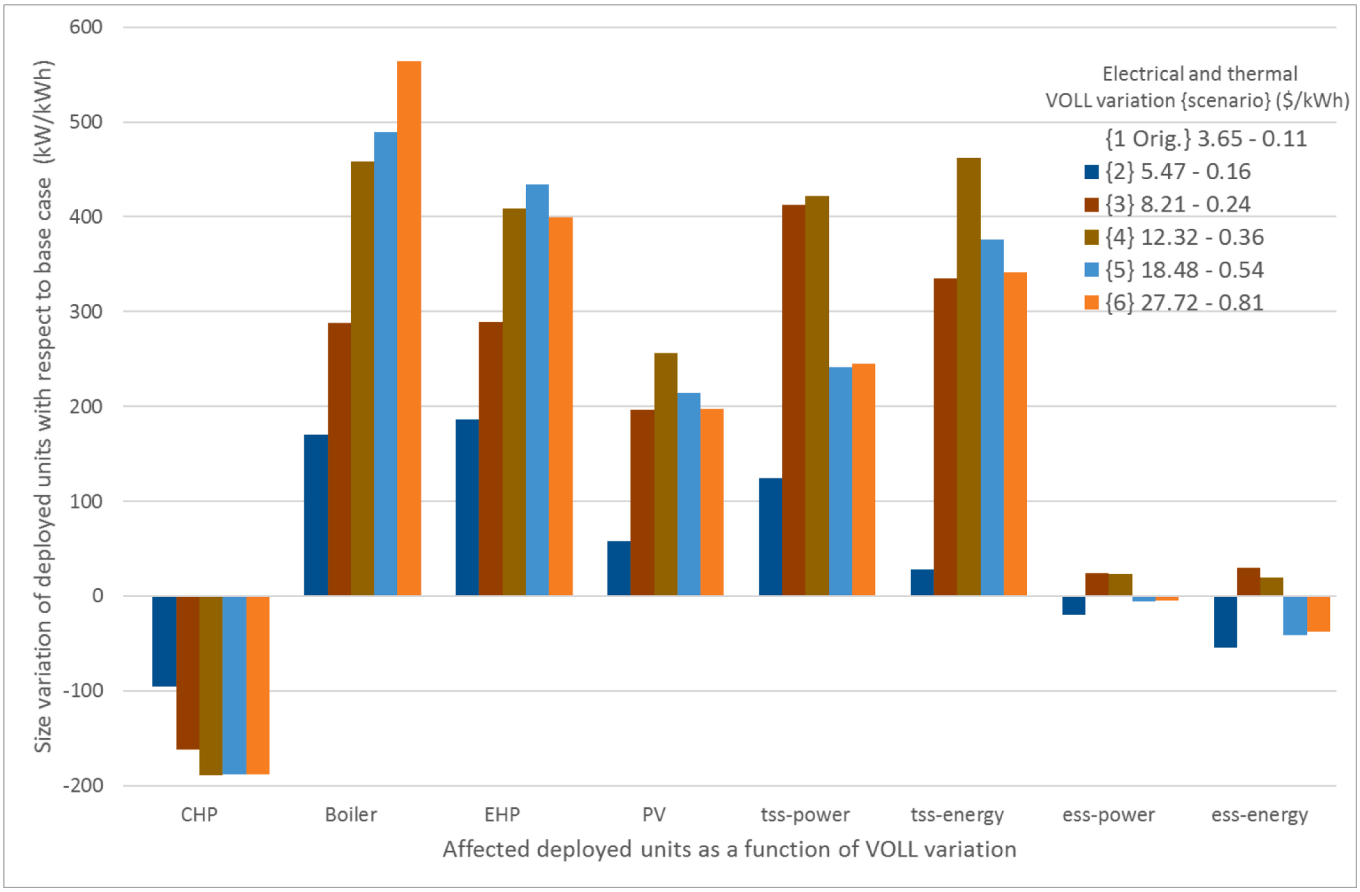

Fig. 8. Impact of VOLL Variations on the Deviation of the Sizing of the Units with respect to the Baseline Scenario.

(26). The amount of energy in-store in each energy storage device at each time-step equals its value in the previous time-step adjusted for self-discharge plus the time-step-wise charging power and minus the time-step-wise discharging power Eq. (21)). Also, the energy stored in each energy storage device at the end of each day is enforced to be equal to its value at the beginning of the day for balanced analysis (Eq. (22)). Furthermore, the hourly charging and discharging power of the storage system cannot exceed its corresponding optimized capacity (Eq. (23)). Moreover, the amount of energy in-store is limited by Eq. (24) considering the depth of discharge. Additionally, the constraints in Eqs. (25)–((26) model the annual throughput of the battery – as the total amount of energy the battery can be expected to store and deliver over one year.

$$E_{uysdh} = \left(E_{uysd(h-1)} - E_{uysdh}\cdot\alpha_u^{loss} + P_{uysdh}^{ch} - P_{uysdh}^{dch} \Big/ \alpha_u^{ef}\right)\cdot A_u \qquad \forall u \in S \tag{21}$$

$$E_{uysd(h1)} = E_{uysd(h24)} \qquad \forall u \in S \tag{22}$$

$$0 \le P_{uysdh}^{dch/ch} \le P_u^{\max}\cdot\left(1 - I_{uysdh}^{attack}\right) \qquad \forall u \in S \tag{23}$$

$$E_u^{\max}\cdot(1 - DOD_u) \le E_{uysdh} \le E_u^{\max} \qquad \forall u \in S \tag{24}$$

$$Thr_{uy}^{annual} = \sum_s\sum_d \mu_{sd}\cdot\sum_h\left(P_{uysdh}^{ch} + P_{uysdh}^{dch} \Big/ \alpha_u^{ef} + E_{uysdh}\cdot\alpha_u^{loss}\right) \qquad \forall u \in ess \tag{25}$$

$$Thr_{uy}^{annual} \le E_u^{\max}\cdot Thr_u \Big/ EL_u \qquad \forall u \in ess \tag{26}$$

2.4. Capacity limit constraints of distributed energy resources

The optimum power and energy capacities of the MCMG's units cannot exceed the associated minimum and maximum allowable values, as expressed in Eqs. (27) and (28), where the binary variable I_u^{inv} is used to indicate the investment state of DERs.

$$\underline{P_u^{cap}}\cdot I_u^{inv} \le P_u^{\max} \le \overline{P_u^{cap}}\cdot I_u^{inv} \qquad \forall u \in \{G, W, S\} \tag{27}$$

$$\underline{E_u^{cap}}\cdot I_u^{inv} \le E_u^{\max} \le \overline{E_u^{cap}}\cdot I_u^{inv} \qquad \forall u \in S \tag{28}$$

2.5. Networks' constraints

The amounts of exchanged electricity and natural gas with the utility networks are, respectively, constrained by the corresponding maximum allowable capacities in Eqs. (29) and (30). The constraint in Eq. (29) also considers a binary variable for the electric utility network's outage and the islanded mode of operation of the MCMG.

$$\left|P_{ysdh}^{Net,e}\right| \le \overline{P^{Net,e}}\cdot I_{ysdh}^{Net,e} \tag{29}$$

$$0 \le P_{ysdh}^{Net,g} \le \overline{P^{Net,g}} \tag{30}$$

2.6. Reliability constraints

A load shedding scheme is utilized to ensure the balance of power between the generation and consumption sides of the MCMG, as expressed in Eq. (31). Given the large VOLL assigned to critical loads, the model inherently seeks to minimize the value of unserved critical loads. The equivalent loss factor is employed to measure the reliability of the MCMG (Eq. (32)). The equivalent loss factor of the MCMG is constrained to be lower than a specific value (Eq. (33)), less than 0.01% per year.

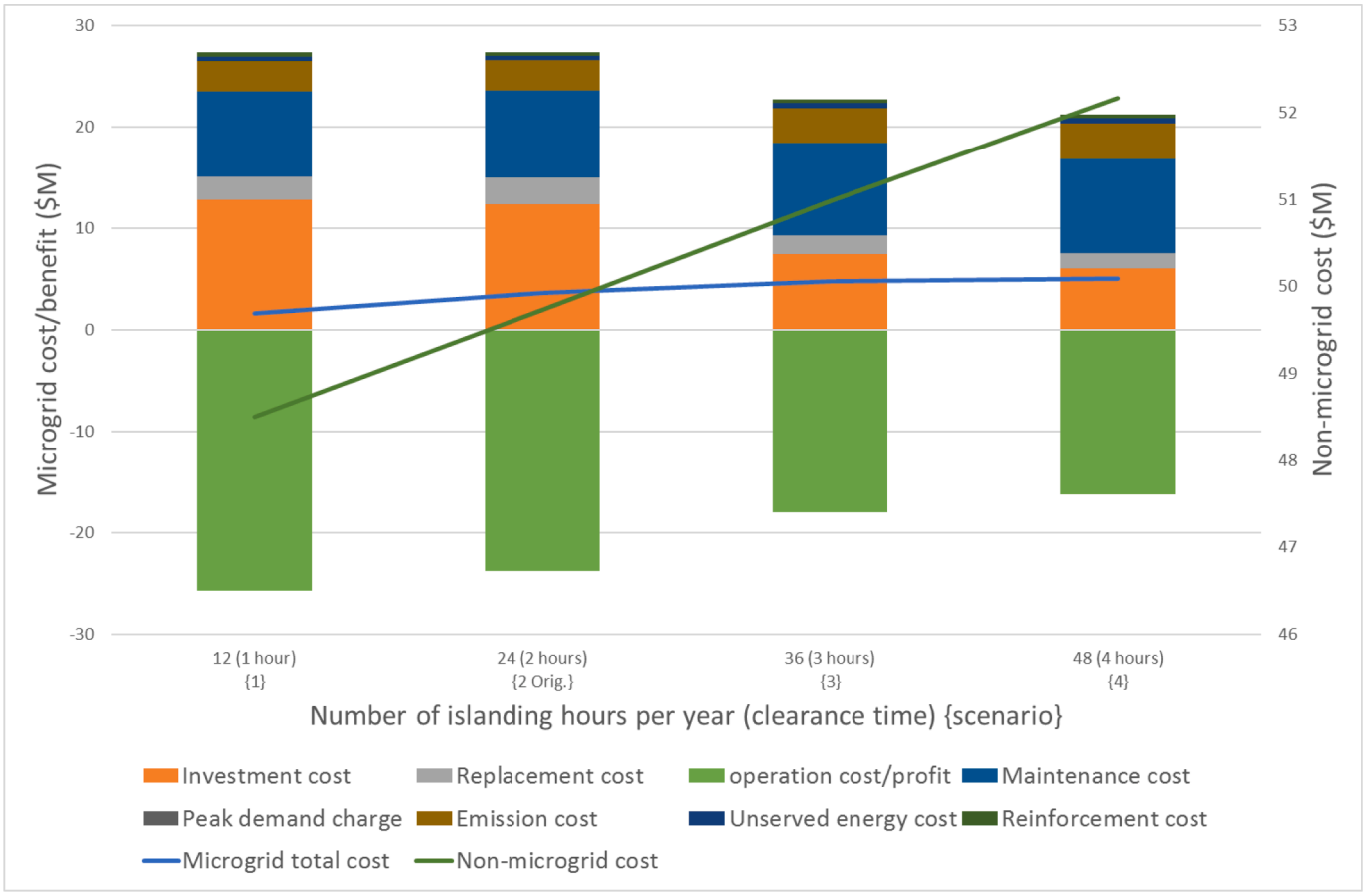

Fig. 9. Breakdown of the Optimal Planning Cost of the MCMG for Various Islanding Hours.

$$0 \le P^{ens,l}_{ysdh} \le D^{l}_{ysdh} \cdot \left(1 - \varphi^{l}\right) \qquad \forall l \in \{e,t\} \tag{31}$$

$$ELF_y = \frac{\left(\sum_s \sum_d \mu_{sd} \cdot \sum_h P^{ens,e}_{ysdh} \Big/ D^{e}_{ysdh}\right)}{N_h \cdot \sum_s \sum_d \mu_{sd}} \tag{32}$$

$$ELF_y \le \overline{ELF_y} \tag{33}$$

2.7. Capital investment constraint

Typically, any MG development project has a budget limit. To reflect this in the model, the total investment cost of the MCMG project is limited by the available capital investment fund (CIF) (Eq. (34)).

$$TIC = IC_y + \mathbb{RC}_y \le CIF \qquad \forall y = 1 \tag{34}$$

2.8. Attacker's budget to trigger disruptions

The annual financial resources for triggering outages in a MCMG's physical units are limited annually, as expressed in Eq. (35). The required financial resource to decrypt and manipulate an encrypted data packet is assumed to be ψ times of the associated encryption cost (Eq. (36)). Also, the period of disturbance and the associated service restoration of disrupted physical units is assumed to be one hour for each attack since the operator of the MCMG could immediately initiate the restoration process.

$$\sum_s^{N_s} \sum_d^{N_d} \sum_h^{N_h} \sum_{u \in \{G,W,S\}} M_u(\varepsilon_u) \cdot I^{attack}_{uysdh} \le Bud^{attacker}_{y} \tag{35}$$

$$M_u(\varepsilon_u) = CR_u(\varepsilon_u) \cdot \psi \qquad u \in \{G,W,S\} \tag{36}$$

2.9. Resilience index

To quantify the vulnerability of the MCMG against intentional disruptions, a resilience index (Eq. (37)) is defined as the exponential of the negative ratio of the increase in the MCMG's overall cost as a result of disruptions due to attacker-budget-aware cyber-attacks. The lower the resilience index, the more vulnerable the MCMG to cyber-physical attacks.

$$RI = e^{-\left(\left(OF^{attack} - OF^{normal}\right) / \left(Budget^{attacker}_{y} \cdot N_y\right)\right)} \tag{37}$$

2.10. Overview of the proposed method

Fig. 1 illustrates the solution algorithm for the proposed two-stage cyber-attack-resilient MCMG planning optimization model, which is able to adequately handle the associated conflicting objectives – total discounted energy planning cost minimization and total cyber-attack-induced disruption maximization. The upper stage determines the optimal planning and scheduling results under normal operating conditions. The results of the upper-stage problem then serve as input parameters to the lower-stage optimal resilience improvement problem, which optimizes the costs associated with the reinforcement of the multi-carrier microgrid against intentional cyber intrusions. The formulated microgrid capacity reinforcement problem, which seeks to optimize the operational cost of the MCMG during attacks, is then solved iteratively using a specifically developed algorithm, which identifies and reinforces the vulnerable units until a resilience index of 1.0 is achieved – as the stopping criterion.

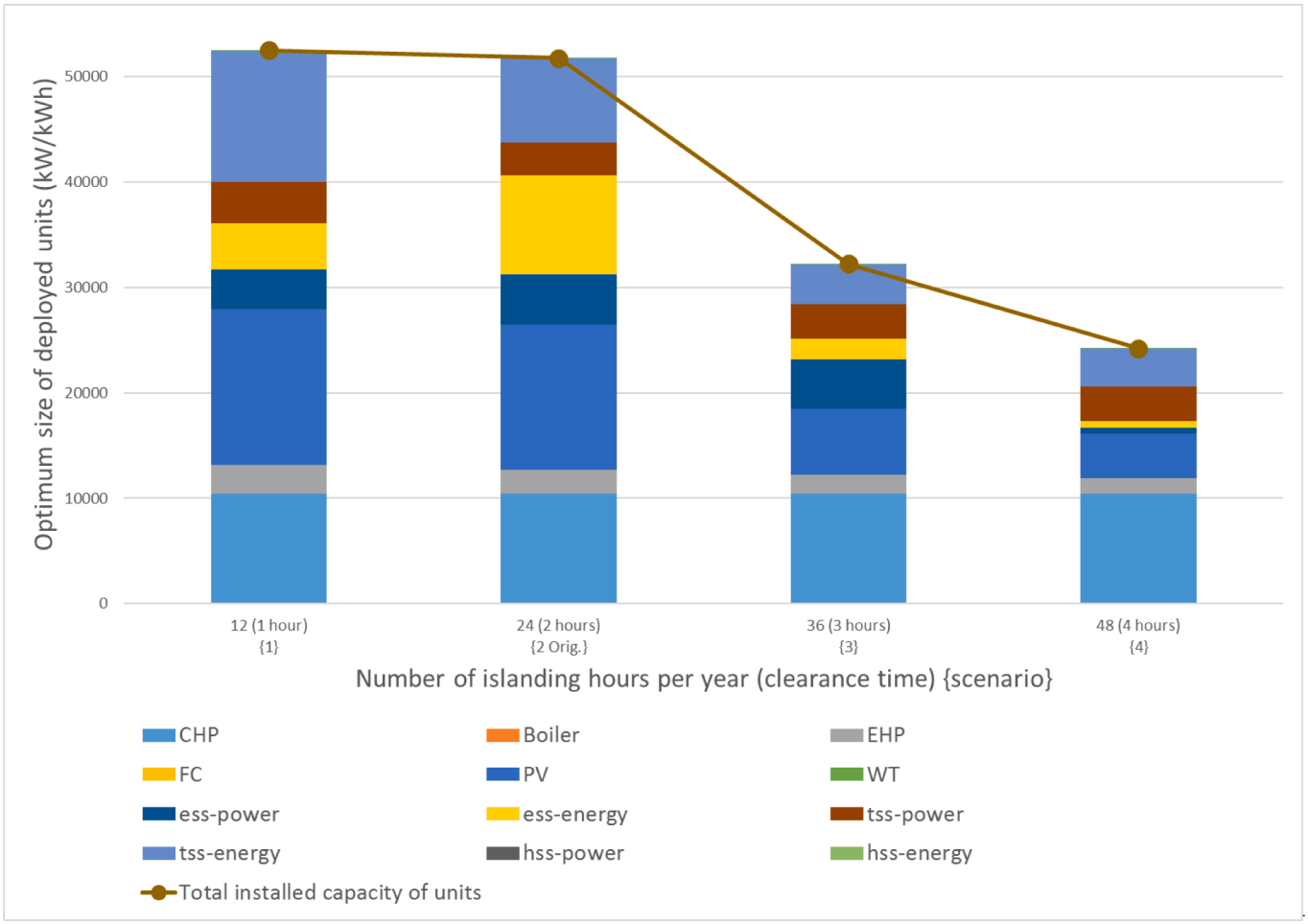

Fig. 10. Impact of the Islanding Hour on the Optimum Size of the Selected MCMG Technologies.

3. Numerical simulations and discussions

As a test-case MCMG, a real-world industrial park located in Golpayegan, Iran (33°32′55.86′’ N, 50°18′02.12″ E) is considered. Tables 1 and 2 present the technical specifications of the candidate DGs and energy storage units, respectively. It is noteworthy that the size of the anaerobic reactor-reformer unit is fixed *ex-ante* and does not form part of the optimal sizing model. Accordingly, the size of the reactor-reformer system is calculated based on the available municipal solid waste in the industrial park, which equates to 20 kW-H_2 per hour. The aggregated electrical and thermal loads on the MCMG are depicted in Fig. 2. Recall that a typical weekday and a typical weekend of the three typical seasons – summer, spring/autumn, and winter – are selected to represent the whole year. The hourly electricity market price retrieved from an online database (ISO-NE, 2015) is presented in Table 3. A fixed natural gas market price of $0.00344/kWh, based on the Henry Hub Natural Gas dataset (U.S. Energy Information Administration, 2016), is utilized in this paper. The power exchange of the MCMG with the wider utility grid is subject to a line capacity limit of 5 MW. Other techno-economic specifications of the project are presented in Table 4. Additionally, the site of interest has an average seasonal (summer, transitional, and winter) ambient temperature of 23 °C, 12.5 °C, and 1.2 °C, respectively, over summer, autumn/spring, and winter, solar irradiance of 580 W/m^2, 483 W/m^2, and 406 W/m^2, respectively, over summer, autumn/spring, and winter, and a wind speed of 5.8 m/s, 4.83 m/s, and 4.06 m/s, respectively, over summer, autumn/spring, and winter, which are collected from the RETScreen Climate Database (U.S. Energy Information Administration, 2020). The planning horizon is also assumed to be 25 years. Moreover, a total annual average of 24 h of operation in the islanding mode were considered, in compliance with historical outage data collected from the Golpayegan Electric Utility Company. The formulated problem was modeled as a mixed-integer programming problem and solved using the GAMS 24.1.2 software (GAMS Development Corp, 2018). The following cases are studied:

Case 1: Resilient MCMG planning analysis considering changes in the capital investment budget;

Case 2: Impact analysis of the value of the lost load on the costing and configuration of the MCMG; and

Case 3: Impact analysis of islanding on the costing and configuration of the MCMG.

Case 1: The optimal cyber-attack-resilient designing of the MCMG populated for the case of interest is carried out using the proposed model for a variety of investment budgets. The optimum capacities of DERs for different values of CIF are displayed in Fig. 3. Also, the share of each unit in the total installed DER capacity is depicted in Fig. 4 for a better understanding of the portfolio-side results. The optimal sizing results indicate that, given the low natural gas prices present, the CHP unit constitutes the largest share in supplying electrical and thermal loads. As shown in the figure, the size of the CHP unit remains practically unchanged for CIF values of greater than $3.56 m, past which it starts to make up smaller percentages of the total DER capacity. Furthermore, for CIF values greater than $3.56 m, the optimal design solution incorporates a large PV unit and a relatively small WT unit due to the climatic conditions of the site of interest, which offers the opportunity of selling the surplus PV generation back to the utility during higher-priced afternoon peak hours. Based on the above observations, an interesting

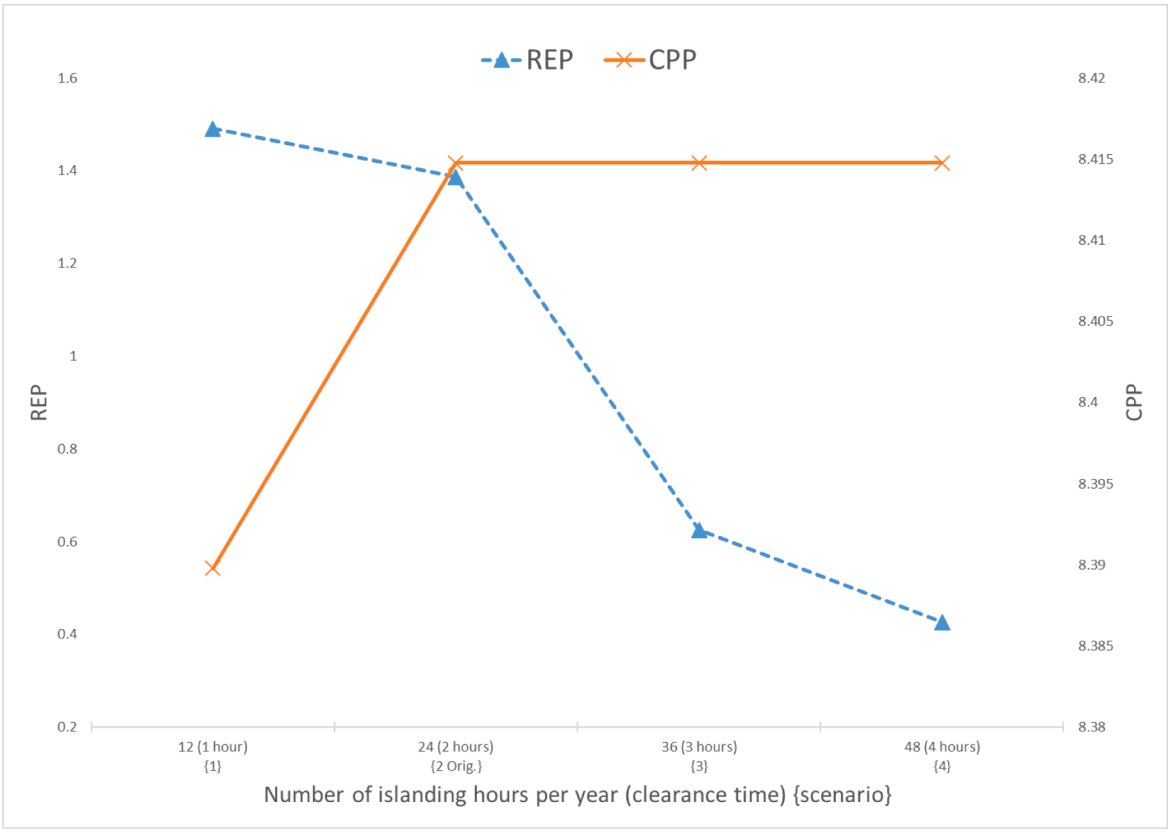

Fig. 11. Impact of the Islanding Hour on the REP and CPP.

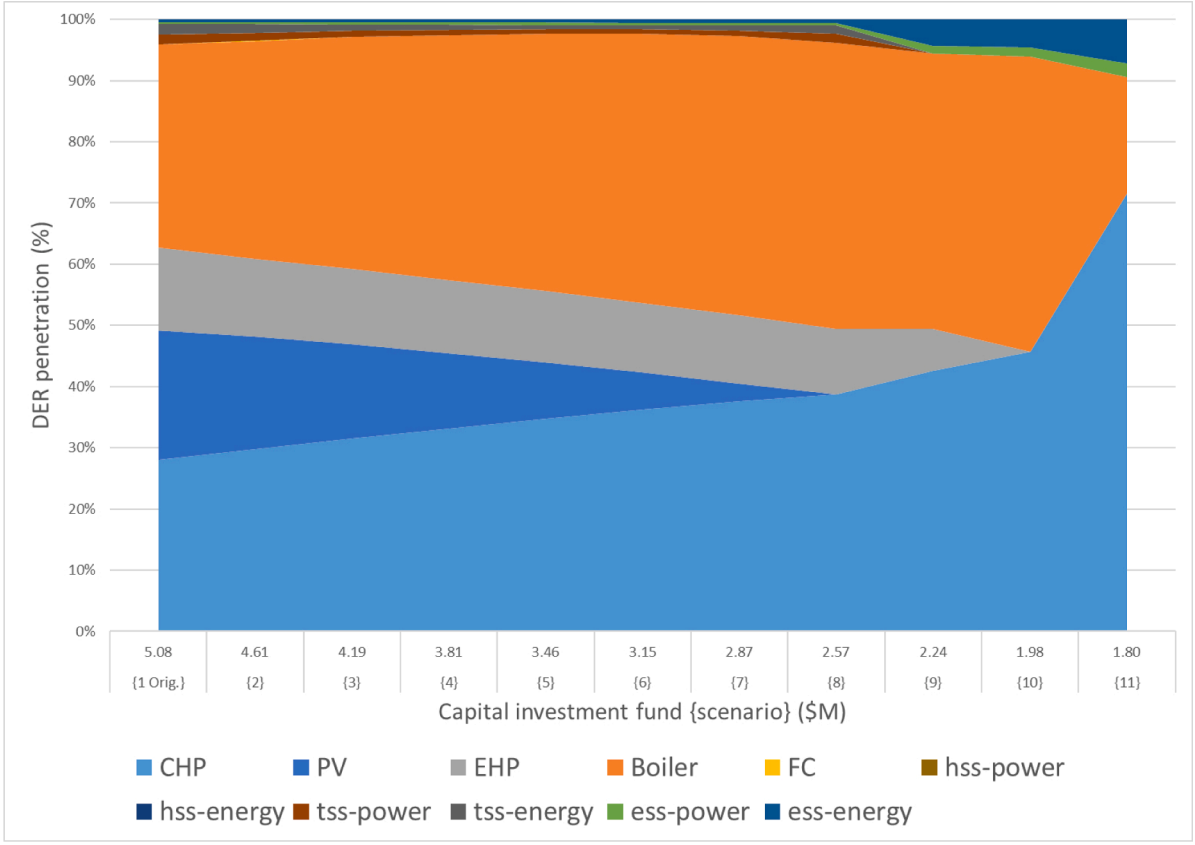

Fig. 12. Optimized Units' Penetration as a Function of CIF in the Islanded Mode Operation Scenario.

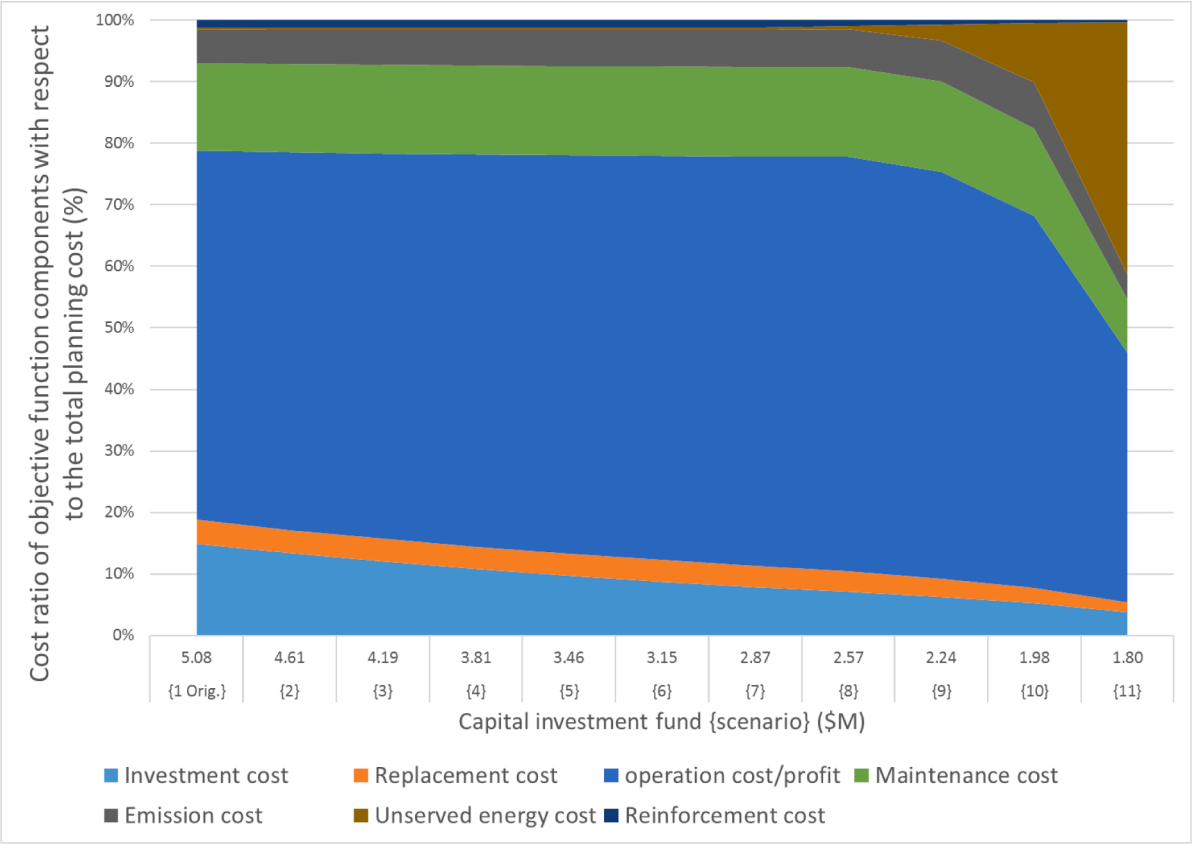

Fig. 13. Breakdown of the Total Cost of the MCMG in the Islanded Operation Mode.

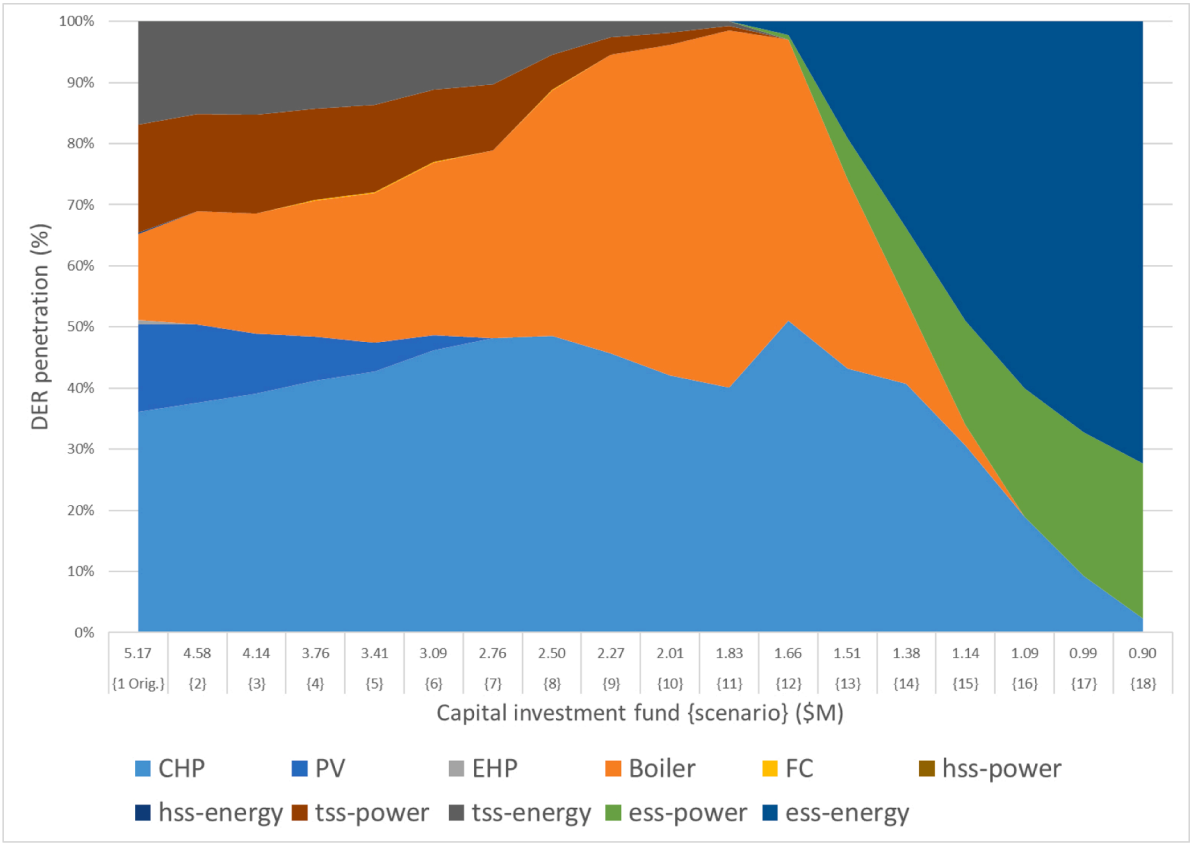

Fig. 14. Optimized Units' Penetration as a Function of CIF in the Increased Electricity Market Price and Reduced Feed-in-Tariff Scenario.

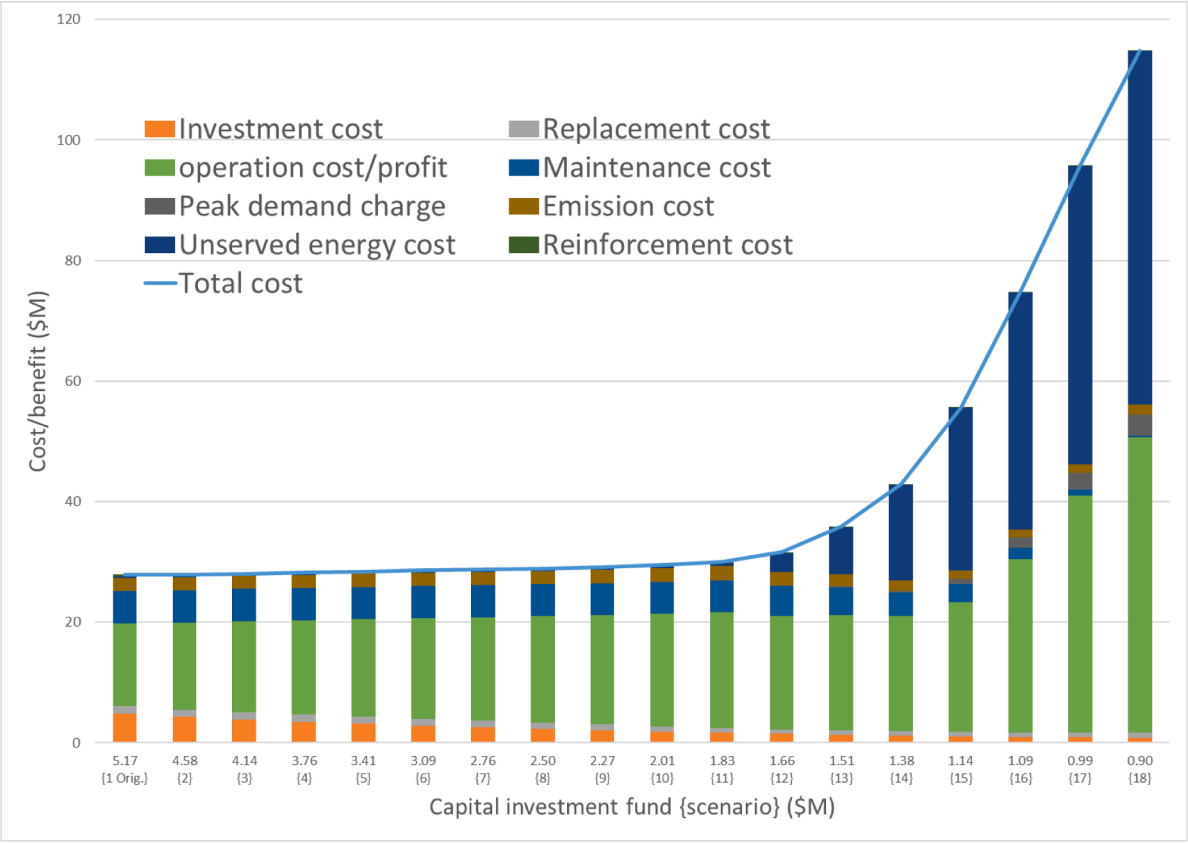

Fig. 15. Breakdown of the Total Cost of the MCMG in the Increased Electricity Market Price and Reduced Feed-in-Tariff Scenario.

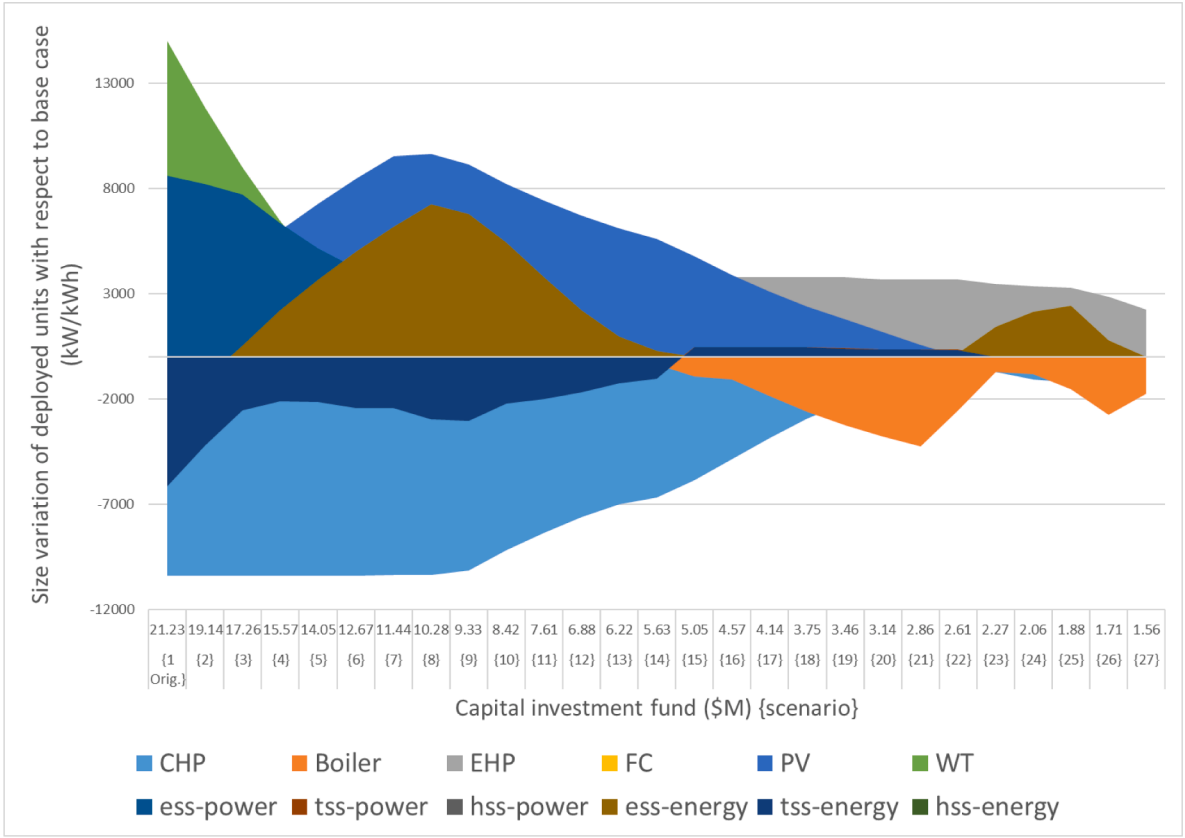

Fig. 16. Impact of a Significant Increase in the Natural Gas Prices on the Optimal Size of the Components.

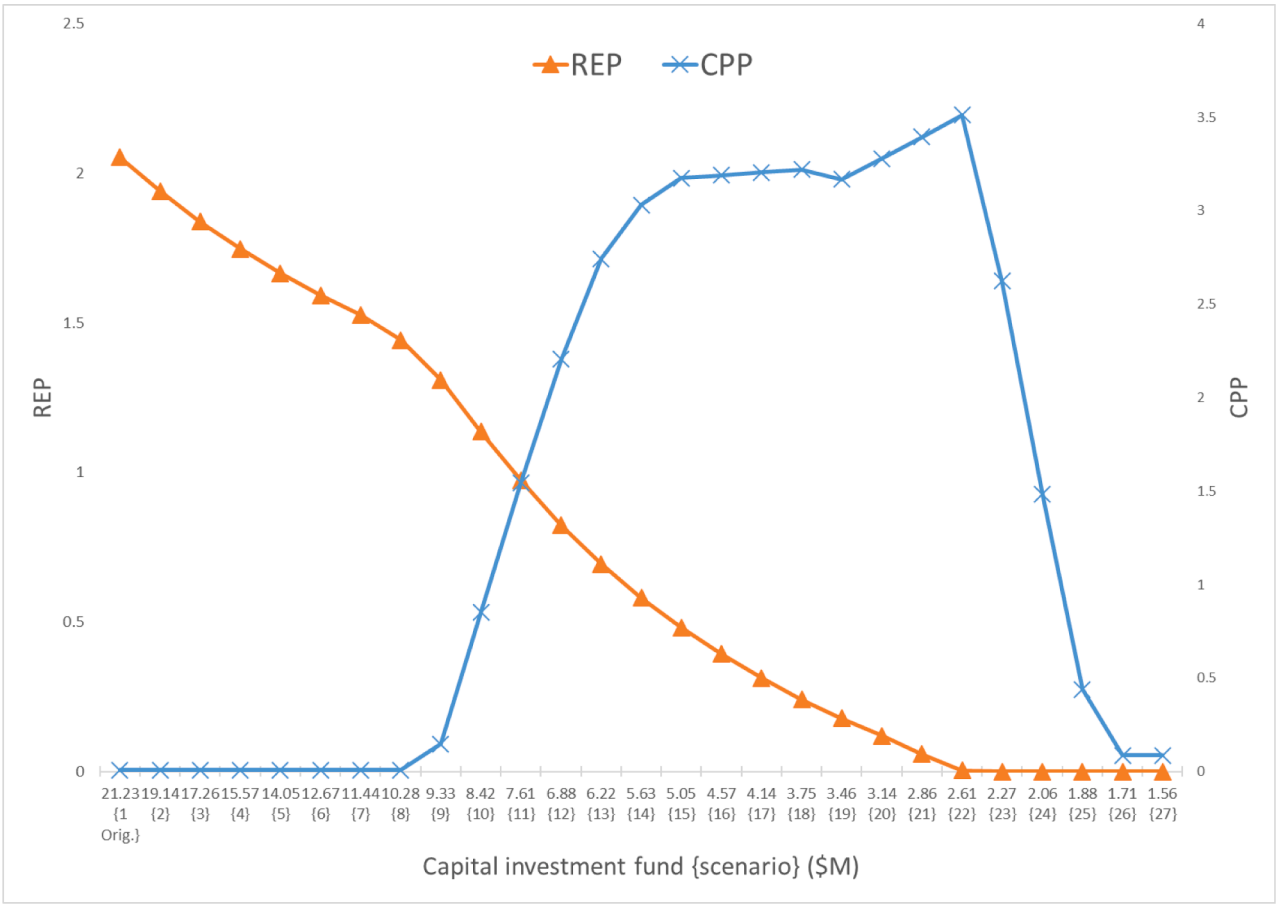

Fig. 17. Impact of a Significant Increase in the Natural Gas Prices on the REP and CPP.

finding is that the financial viability of solar PV installations is subject to the availability of higher capital resources, especially given the necessity of adding capital cost-intensive storage systems and dispatchable DGs.

The results also indicate the comparatively lower size of the FC given the available hydrogen production capacity from municipal solid waste. That is, hydrogen storage is a viable option only where abundant municipal solid waste exists. Furthermore, for the CIF values in the range $3.56 m–$12.72 m, the optimal planning solution is to install a thermal storage system (TSS) to assist the provision of the heat demand. The determined energy rating of the TSS is found to be 2.53 times its power rating for a non-constrained CIF scenario. However, the more limited the capital budget, the lower the energy rating of the TSS. In addition, although the model behavior with respect to the size of the electrical storage system (ESS) planning decision is almost similar to that of the TSS in terms of the capital budget-wise allocated capacity, the baseline size of the ESS is substantially larger than the TSS given the important dynamics that take place with respect to the on- and off-peak electricity prices. More specifically, the ESS energy rating is calculated to be around 1.19–1.95 times of its power rating for CIF values of $5.78–$12.72 m, and around 2.86 times of its power rating for CIF values lower than $1.47 m. Another insight is that the ESS makes up around 22–86% of the total installed capacity of MCMG-wide DERs for CIF values in the range $1.47–$1.02 m – that is, the lower the CIF, the greater the portfolio share of the ESS. Moreover, in addition to the components that contribute to the provision of both electrical and thermal loads, a medium-sized EHP and boiler are allocated as auxiliary heat production components. The results also indicate the EHP utilization ratio increases sharply for CIF values larger than $6.43 m, whereas the boiler is a better option for more limited capital budgets. The results collectively indicate the importance of dispatchable DGs, as well as electrical and thermal storage units, to ensure an uninterruptable supply of demands and provide economic benefits for MCMG investors.

Fig. 5 shows the breakdown of the total MCMG planning cost optimized for different CIF values. The total cost of the MCMG varies with three constant slopes with respect to the CIF parameter. More specifically, the three constant slopes for changes in the total system cost with respect to the CIF represent the capital cost ranges $12.72–$3.09 m, $3.09–$1.56 m, and $1.56–$1.02 m, which are equal to 0.401, 11.694, and 97.623, respectively. Furthermore, reducing the maximum allowable CIF from $12.72 m to $3.56 m reduces the discounted operational cash inflows by about 5.4% in each scenario, while increasing the operation and maintenance costs by an insignificant 0.9%. A further decrease in the CIF results in a sharp decrease in the operational cash inflows, which ultimately fall to zero for the CIF value of around $2.3 m. Also, imposing such an extreme limitation on the CIF results in a considerable rise in the operation and maintenance cost of the MCMG from the original $0.33 m to $31.63 m.

According to Fig. 5, decreasing the CIF from $12.72 to $1.02 m leads to an initial slight rise, followed by a steep decline in the emissions cost factor of the total system cost. The emissions cost factor also exhibits an erratic behavior in some intervals given the optimal system dynamics that are taking place with respect to the size of the gas-fired units. Furthermore, the peak demand charge is equal to zero for CIF values of greater than $1.72 m, implying the customers would prefer to purchase electricity from the wider utility grid at any (reasonable) cost, rather than experiencing power outages. Also, the cost of unserved energy associated with a partial curtailment of low-priority thermal loads increases from $0.43 to $2.03 m by limiting the CIF from $12.72 to $1.89 m; the cost of unserved energy is more substantial for the scenarios where the CIF is lower than $3.09 m due to the inadequate size of the

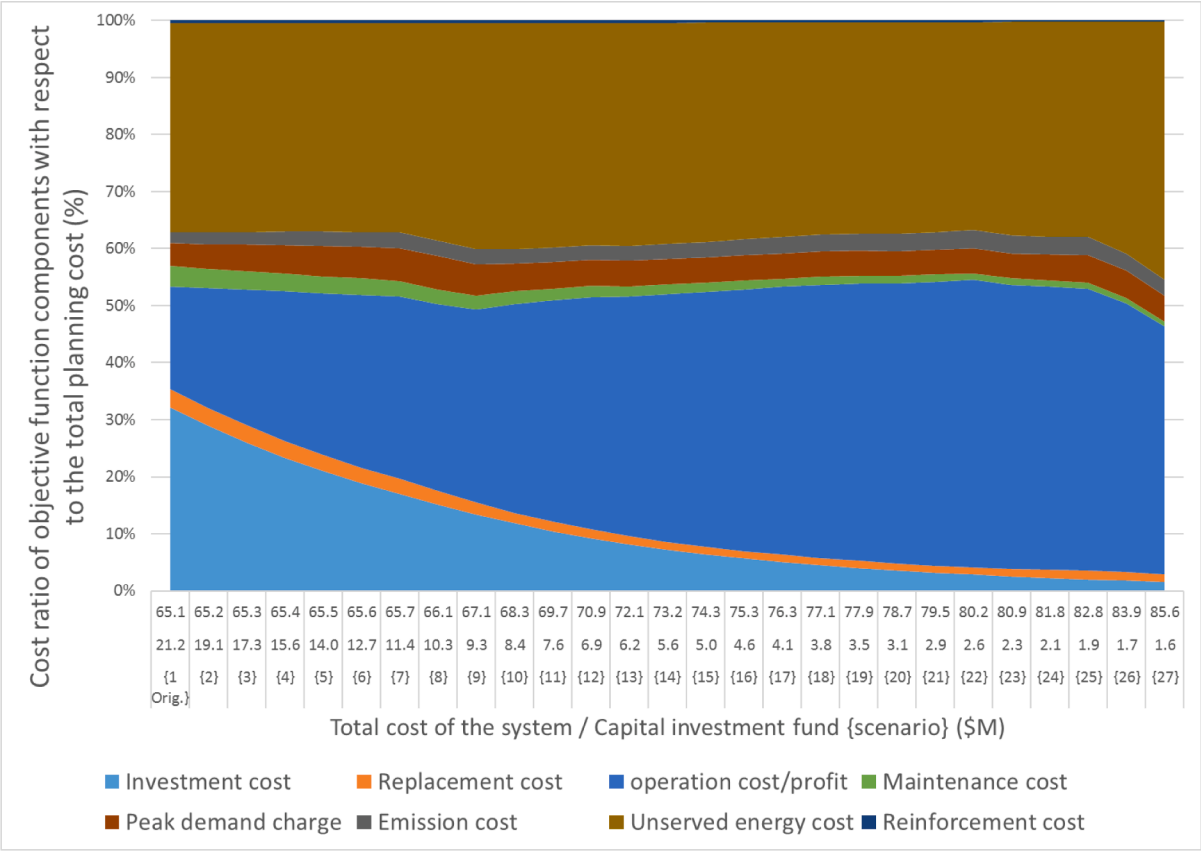

Fig. 18. Breakdown of the Total Cost of the MCMG in the Increased Natural Gas Price Scenario.

CHP unit. Limiting the CIF to a greater extent (lower than $1.89 m) results in a very large unserved energy cost (which constitutes 10–47% of the total planning cost) as a result of the necessity of higher-priority electrical demand curtailment. In addition, the reinforcement cost makes up about 0.2–9.7% of the total planning cost; the more the capital budget, the lower the reinforcement cost due to the increased diversity of the portfolio necessary for energy security. Collectively, the results indicate that the economic viability of the MCMG system populated for the case of interest is ensured for CIFs greater than $2.53 M given that the accrued revenues outweigh the investment costs.

To evaluate the technical viability and financial sustainability of the project proposal, several metrics including the levelized cost of energy (LCOE) (Adefarati & Bansal, 2019), the discounted payback period (DPP) (Mohseni et al., 2019), and the profitability index (Mohseni et al., 2019), the renewable energy penetration (REP) (Amir & Azimian, 2020), the conventional power penetration (CPP) (Amir & Azimian, 2020), the purchase probability (PP) (Amir & Azimian, 2020), the sale probability (SP) (Amir & Azimian, 2020), as well as various reliability indices such as the loss of load expected (LOLE), the loss of load probability (LOLP), loss of energy expectation (LOEE), and loss of power supply probability (LPSP) (Pazouki, Haghifam & Moser, 2014), are used.

The impact of changes in the CIF on the capital budgeting metrics of the planned MCMG is summarized in Fig. 6. As the figure shows, decreasing the CIF from $12.72 to $1.02 m significantly affects the financial viability of the project. More specifically, as the capital budget decreases, the discounted payback period of the project does so as well, though not strictly necessarily. However, the LCOE is a strictly increasing function of the CIF. Additionally, changes in the profitability index indicate that the profitability of the project is a strictly increasing function of the CIF for CIF values greater than $1.34 m, below which the profitability index is reduced significantly. It should be noted that a profitability index greater than 1.0 indicates that the project's cash inflows are expected to exceed the project's cash outflows, and therefore it generates profit. Moreover, the LCOE of the project was found to lie within the range of $0.00106/kWh–$0.06161/kWh for CIF values greater than $1.11 m. This further verifies the economic viability of the MCMG project proposal in view of the fact that the present average tariff rate at the case study is $0.086/kWh.

Table 5 details the results obtained for various reinforcement levels of the MCMG's units against cyber-attacks – as part of the overall iterative resilient planning process – for different CIF value scenarios. More specifically, the proposed process, first, identifies the most vulnerable units that would be the primary targets of attackers, and then reinforces them in the next iteration. Accordingly, it proceeds by prioritizing the identified units at each iteration for further reinforcements in the next iteration until an acceptable level of resilience is achieved. It should be noted here that the total cost of the MCMG under normal operating conditions (resilience index = 1) is estimated to be $3.61 m.

The results presented for scenario 1 in Table 5 indicate that the intentional attack results in the disruption of CHP and PV units in the first iteration, with a consequent 26% increase in the total cost of the MCMG compared to the normal operating conditions. Accordingly, the total cost increases from $3.61 m in the baseline scenario to $4.56 m. It is noteworthy that the weakest encryption strategy for the units under consideration is applied in iteration 1, which accounts for around 2.04% of the total cost. However, the encryption strategy in iteration 2 is more sophisticated, and entails the reinforcement of the attack-prone units – identified in the previous iteration – which makes up about 3.04% of the total cost. Interestingly, the encryption strength of each vulnerable unit is found to be double the initial encryption strength. The results of the second iteration indicate that the CHP and PV units are attacked again and the ESS is additionally disrupted. Additionally, the total cost of the project is reduced by 14% to $3.93 m in iteration 2 compared to iteration 1. Also, the reinforcement cost in iteration 3 is increased to $0.19 m

from $0.12 m in iteration 2, while the total cost is reduced by 8% compared to the previous iteration. Given that the CHP and PV units are under more surveillance – given the identified and nullified attacks in the previous iterations – the electrical and thermal storage units are identified to be the primary targets for disruption in iteration 3. The associated minimum total cost is yielded in the fourth iteration of the reinforcement process, which shows $0.1 m of savings compared to the baseline scenario. In iteration 4, the total cost is found to be $3.51 m, with an associated resilience index of around 0.99, which is deemed sufficient. That is, any further reinforcement of the MCMG's assets to reach a resilience index of greater than 0.99 is associated with high encryption costs for low-probability, low-impact attacks, thereby impairing the economic viability of the project. More specifically, the best trade-off between resilience and cost is selected to be the iteration where the sum of the planning and reinforcement costs is minimum. Underlying this choice was the insight that as the reinforcement cost increases, the planning cost decreases due to the improved encryption strength of the selected physical units and minimized costs of unserved energy. Another insight is that the best compromise solution is highly dependent on the chosen CIF.

Further insights into the assets that are more prone to cyber-attacks in the resulting infrastructure mix of the MCMG are necessary for informed prioritization decisions. Fig. 7 shows the percentage frequency of the intentional cyber disruption of the relevant components, in accordance with the best trade-off solutions. The figure indicates the following rank order for the probability of outage of the components prone to attacks: the CHP unit (41.94%), the PV plant (20.16%), the ESS (19.35%), the boiler (8.06%), the TSS (6.45%), the EHP (2.42%), and the FC (1.61%).

Case 2: In this case, the effects of changes in the VOLL on the planning results are studied for an unlimited CIF. Fig. 8 illustrates the effect of VOLL variations on the deviation of the sizing of the units with respect to the baseline scenario (Orig. 1). It can be observed that higher VOLL values result in a modest decrease in the size of the CHP unit. However, the size of heat generators, including the boiler and EHP, supported by the TSS and CHP systems undergo a more dramatic change to uninterruptedly meet the heat demand. An important insight is that there exists a turning point for the size of the TSS, which occurs where the penetration level of heat generators exceeds a certain amount. Furthermore, the penetration of the CHP unit is found to be inversely correlated with the size of the PV unit. The direct correlation of the size of the PV plant and the ESS also indicates that the variability of the PV plant is addressed mainly by the ESS.

In terms of the impact on the curtailed loads, the results indicate that increasing the VOLL results in relatively insignificant changes in the curtailed loads, and consequently the total penalty of unserved energy. More specifically, the total cost increases around 11% from $3.61 m to approximately $4 m in the extreme case where higher VOLL for electrical and thermal loads is greater than $12.32/kWh and $0.36/kWh, respectively.

Another observation is the sensitivity of the capital budgeting metrics to changes in the VOLL. More specifically, the results indicate a reduction of around 1 year in the DPP of the project in the above-mentioned extreme VOLL case, with an associated 33% increase in the profitability index, despite higher total costs, which can be primarily attributed to the 34% savings generated from the avoided lost loads' penalties. This indicates that the VOLL plays a key role in the economic viability evaluation of MCMG systems.

Case 3: In this case, the optimal MCMG planning problem with a boundless CIF is solved for various multi-period islanding scenarios – islanding modes that continue for several hours. The total planning cost of the MCMG and its breakdown are shown in Fig. 9 for various islanding hours. The figure also presents the associated total operational cost of meeting the loads without implementing the proposed MCMG through grid imports (denoted by non-microgrid costs). As the figure shows, increasing the number of islanding mode operation hours for cyber-attack-induced interruptions that last from 12 to 48 h per year increases the non-microgrid operational cost and the optimal MCMG planning cost by 8% and 211%, respectively. The figure also reveals that increasing the islanding hours decreases the accumulated operational cash inflows by 37%, but substantially increases the emissions costs and unserved energy costs; specifically, by 18% and 20%, respectively. It has also been found that increasing the total duration of outages from 12 to 48 h reduces the DPP from 6 years to 4 years, whilst additionally improving the profitability index by 113%, from 3.66 to 7.8.

The impact of the number of islanding hours on the DER sizing and REP level is depicted in Figs. 10 and 11. As Fig. 10 shows, the total optimal capacity of generation units is approximately halved, from 52.5 to 24.2 MW, by increasing the islanding hours from a total of 12 h per year to a total of 48 h per year in intervals of 12 h. This has also decreased the optimal size of the EHP unit by 45%, from 27.4 MW to 15 MW. Consequently, the optimal energy rating of the TSS is reduced by a significant 86% in view of the fact that the optimal energy rating of the TSS reaches close to the associated power rating. Furthermore, the optimal PV unit capacity is reduced by 71%, which has consequently resulted in the reduction of the energy and power ratings of the ESS by a similar 86%. Moreover, the most notable insight emerging from Fig. 11 is that increasing the number of islanding hours to a total of 48 h per year (i.e., 12 events each taking 4 h) from the original total of 12 h per year (i.e., 12 events each taking 1 h) decreases the REP to 43% from 149%, whilst simultaneously increasing the CPP by around 1 min. The above discussion indicates that the economic viability of the MCMG is highly dependent on the number of multi-period islanding events per year. More specifically, a larger number of islanding events results in lower revenue streams for the MCMG's investors.

To corroborate the effectiveness of the proposed model and demonstrate its robustness to changes in input values, further scenario analysis were carried out considering the following cases: (i) islanded mode operation, (ii) increased electricity market prices and reduced feed-in-tariff, as well as (iii) increased natural gas market price.

Islanded mode operation: In this scenario, it is assumed that the MCMG is entirely disconnected from the wider power utility network and electricity is solely provided by local resources. However, the natural gas network is assumed to be available. The results of the optimized units' penetration as a function of CIF in this scenario are presented in Fig. 12. As the figure shows, the most economically viable local units for power generation are the CHP unit and the solar PV plant with the thermal loads mainly supplied by the boiler, and in lesser part by the electric heaters. The results also indicate that when the capital budget is sufficient, around 40% of the total demand of the industrial park is served by the solar PV plant. However, a reduced budget of $2.24 m leads to a solar PV penetration of around 0.04%. Moreover, from the results, it can be observed that the penetration of the battery storage system is insignificant, with a power capacity in the range 0.3–2.2% and an energy capacity in the range 0.4–7.2% – to effectively handle the mismatches in the supply and demand profiles. Importantly, as the capital budget decreases, the capacity of the battery storage system increases. On the contrary, a relatively small thermal storage capacity has been allocated, which decreases with reductions in the capital fund. In addition, the total power generation capacity is in the range 6.7–18.4 MW and the total energy storage capacity is in the range 181.8–518.4 kWh depending on the capital budget.

Also, Fig. 13 shows a breakdown of the total planning cost, namely the investment costs, replacement costs, operational costs (including the fuel import costs), maintenance costs, emissions costs, unserved energy costs, and reinforcement costs in the islanded mode operation. As the figure shows, for capital budgets lower than $2.24 m, the cost of unserved energy is significantly increased due to the shedding of critical loads. Also, the planning cost in this mode ranges from $1.8 to $5.08 m given the level of resilience desired. Additionally, the LCOE is found to be in the range of $0.019/kWh to $0.037/kWh. This shows that even in the islanded mode operation, the LCOE of the system is lower than the

average retail tariff, provided that relatively large capital resources are available.

It is also noteworthy that further unreported analysis identified the total lost load of the MCMG to be equal to approximately 3.18 MWh, which occurs in the last year in the planning horizon (year 25).

Increased electricity market prices and reduced feed-in-tariff: In this scenario, it is assumed that electricity market prices are doubled and the feed-in-tariff is halved. The results of the optimized units' penetration as a function of CIF in this scenario are presented in Fig. 14. As the figure shows, the optimal capacity of the MCMG's local generation resources is approximately halved compared to the baseline scenario, provided that sufficient capital resources are available. This results in a reduction of the excess renewable power generation, and consequently reduced income from electricity exports. More specifically, the optimal capacity of the solar PV plant is approximately 5 times lower than that of the baseline scenario. Also, the main power and heat generation resources are the CHP unit and the boiler, respectively, with specifically allocated thermal storage to store the excess heat generation of the CHP unit. However, when the capital fund is lower than $1.83 m, the optimal result is to allocate larger capacities of battery storage to meet critical loads uninterruptedly. However, no extra capacity is specifically allocated to uninterruptedly meet thermal loads. Accordingly, the results reveal that the optimal size of the components, especially those useful for generating a revenue stream from exports, is particularly sensitive to the associated power exchange rates.

Also, Fig. 15 shows a breakdown of the total planning cost, namely the investment costs, replacement costs, operational costs, maintenance costs, emissions costs, unserved energy costs, peak demand charges, and reinforcement costs in the increased electricity market price and reduced feed-in-tariff scenario. As the figure shows, the total operational cost of the MCMG is positive compared to the baseline scenario where it is negative, which indicates that power exchange with the grid incurs costs, rather than generating profits. The reason lies in the combination of the increase in import costs and the decrease in export tariff. Also, the results reveal that the PP is in the range of 12 to 28.7%, while the SP lies in the range of 55 to 60%, which indicates that the MCMG still prefers to export the excess generation, rather than importing the power deficits. It is also noteworthy that the lower the capital budget, the higher the PP, the lower the SP.

The LCOE of the MCMG in this scenario is found to be in the range between $0.0146/kWh and $0.235/kWh. Note that, unlike all other cases, in the last case, where the capital budget is equal to $0.9 m, it is not economically viable to develop the MCMG because the associated LCOE is greater than the average feed-in-tariff by approximately 36%.

It is also noteworthy that further unreported analysis identified that, when the capital budget is lower than $1.83 m, the total lost load of the MCMG is in the range of 3.39 MWh to 5.7 MWh (depending on the budget), which occurs from the 22nd year of the MCMG operation onwards.

Increased natural gas market price: In this scenario, it is assumed that the natural gas market price are increased by a factor of 5. Fig. 16 summarizes the changes in the optimal configuration of the MCMG and the associated optimal size of the components in this scenario compared to the baseline scenario. As the figure shows, the optimal decision is to substantially reduce the optimal capacity of natural-gas-dependent resources, such as the CHP and the boiler, whilst simultaneously increasing the size of renewables. This also entails significantly increasing the size of the electrical heater and the thermal energy storage system. Notably, the optimal capacity of the WT generation unit is significantly increased for the cases where the budget is greater than $11.44 m, despite the fact that the site is less richly endowed with wind resources, which results in lower capacity factors.

Moreover, Fig. 17 depicts the penetration of renewables and conventional generators in this scenario. As the figure shows, for the cases where the capital budget is greater than $7.61 m, the electrical loads on the MCMG is, in larger part, met by the renewables and electricity imports, whereas decreasing the budget results in a decrease in the capacity of onsite renewables with a consequent increased reliance on conventional units. In addition, for the cases where the budget is lower than $2.27 m, the electrical load is mainly met by imports supported by the battery storage system.

Fig. 18 shows a breakdown of the total planning cost into its constituent cost components in this scenario. According to the figure, the planning cost components have undergone a significant change compared to the baseline case. More specifically, the peak demand charges in the scenario with increased natural gas prices make up around 4 to 6% of the total planning cost for different capital fund cases. Also, the operational cost (including the fuel import costs and net electricity imports) comprise 18 to 50% of the total planning cost, while the unserved energy costs (mainly unmet thermal loads) are responsible for a significant 37 to 45% of the total costs, which demonstrate the important impact of natural gas costs on the planning results.

In addition, the results reveal that the PP is in the range of 87 to 92%, while the SP lies in the range of 55 to 60% for different capital budgets, which indicates that the MCMG is seeking to buy the capacity deficits from the wider utility grid to reduce the unserved energy costs.

The LCOE of the MCMG in this scenario is found to be in the range between $0.043/kWh to $0.089/kWh depending on the budget, whereas the profitability index varies between 1.34 to 5.54, which indicates the reduced attractiveness of the project for investment due to the increased natural gas prices.

It is also noteworthy that further unreported analysis identified that the total lost load of the MCMG is in the range of 2.2 MWh to 5.7 MWh (depending on the budget), which occurs from the 21st year of the MCMG operation onwards. This indicates the important role of the CHP in an affordable uninterrupted supply of electrical loads.

4. Conclusion

While the information and communications technologies are necessary for the optimal operation of multi-carrier microgrids, they are exposed to cyber-attacks, which in turn jeopardize the security of microgrids. This indicates the necessity of reinforcing the sensitive assets to ensure a reliable and robust operation of multi-carrier microgrids, and developing a resilience-oriented optimization strategy for an uninterruptable supply of critical loads during the periods of intentional disruptions. In this light, this paper has presented an effective, generic framework for designing resilient multi-carrier microgrids prone to cyber-physical attacks. The proposed modeling framework assists the associated multi-carrier microgrid planning decision-making processes considering the added infrastructure needed to tolerate the cyber-physical attacks and the associated impacts on the total multi-carrier microgrid development costs. The cyber-attack-resilient operation of multi-carrier microgrids, optimized by the proposed method, has also been ensured using a specifically developed preventive reinforcement strategy, which not only identifies the vulnerable distributed energy resources, but also reinforces the most vulnerable assets in a prioritized, systematic way. To this end, the overall problem has been formulated as a mixed-integer programming problem seeking to minimize the total planning cost incorporating the investment, replacement, and operation and maintenance costs of distributed energy resources, peak demand charges, emissions costs, unserved energy costs, as well as the costs associated with the reinforcement of multi-carrier microgrids against intentional cyber intrusions.

The effectiveness of the proposed model has been verified by applying it to a real-world case study. The numerical simulation results have demonstrated the economic viability and resilience benefits of the proposed model using various metrics. A key insight obtained from the numeric simulation results is that reinforcing multi-carrier microgrid systems against cyber incidents results in total cost increases of between 0.33 and 22.87% compared to the baseline case, depending on the encryption strength desired. Also, as far as the results from the case

study are concerned, servicing the aggregated electrical loads of 1.83 MW and thermal loads of 7.2 MW is highly economically viable for capital budget values of greater than $2.53 m, though the project proposal remains attractive for capital budgets in the range of $1.11 m to $2.53 m. Moreover, the role of the battery storage system in the cost-optimal meeting of electrical loads is more salient when the renewable energy penetration exceeds 39%.

While the numeric simulations are carried out for a specific case, the proposed model can be readily adapted for application to other case studies. That is, the proposed resilience-oriented multi-carrier microgrid development model is readily scalable as it comprehensively incorporates the technical, economic, environmental, and practical aspects of energy planning optimization. In addition, the proposed generic mixed-integer programming model can be readily reformulated for different candidate DERs. In conclusion, the proposed model provides three novel generalizations of standard multi-carrier microgrid planning optimization, namely: (i) considerations of cyber-attacks during the planning phases of multi-carrier microgrids can have substantial impacts on the associated business cases, (ii) as the value of lost load increases, the need for cyber-attack-resilient planning of microgrids does so as well, and (iii) as the expected total annual duration of disruptions increases, the share of renewables in the energy mix of cyber-attack-resilient microgrids decreases.

Declaration of Competing Interest

The authors declare that they have no known competing financial interests or personal relationships that could have appeared to influence the work reported in this paper.

References

U.S. Energy Information Administration November 2, 2020 RETScreen n.d. https://www.nrcan.gc.ca/maps-tools-publications/tools/data-analysis-software-modelling/retscreen/7465 (accessed( )).

Adefarati, T., & Bansal, R. C. (2019). Reliability, economic and environmental analysis of a microgrid system in the presence of renewable energy resources. *Applied Energy, 236*, 1089–1114. https://doi.org/10.1016/j.apenergy.2018.12.050

Alsaidan, I., Khodaei, A., & Gao, W. (2018). A comprehensive battery energy storage optimal sizing model for microgrid applications. *IEEE Transactions on Power Systems, 33*, 3968–3980. https://doi.org/10.1109/TPWRS.2017.2769639

Amir, V., & Azimian, M. (2020). Dynamic multi-carrier microgrid deployment under uncertainty. *Applied Energy, 260*, Article 114293. https://doi.org/10.1016/j.apenergy.2019.114293

Amir, V., Jadid, S., & Ehsan, M. (2017). Optimal design of a multi-carrier microgrid (MCMG) considering net zero emission. *Energies, 10*. https://doi.org/10.3390/en10122109

Amir, V., Jadid, S., & Ehsan, M. (2019). Operation of networked multi-carrier microgrid considering demand response. *The International Journal for Computation and Mathematics in Electrical and Electronic Engineering, 38*, 724–744. https://doi.org/10.1108/COMPEL-07-2018-0276

Azimian, M., Amir, V., & Haddadipour, S. (2020a). Microgrid energy scheduling with demand response. *Advances in Energy Research, 7*, 85–100. https://doi.org/10.12989/eri.2020.7.2.085

Azimian, M., Amir, V., & Javadi, S. (2020b). Economic and environmental policy analysis for emission-neutral multi-carrier microgrid deployment. *Applied Energy, 277*, Article 115609. https://doi.org/10.1016/j.apenergy.2020.115609

Bajwa, A. A., Mokhlis, H., Mekhilef, S., & Mubin, M. (2019). Enhancing power system resilience leveraging microgrids: a review. *Journal of Renewable and Sustainable Energy, 11*, Article 035503. https://doi.org/10.1063/1.5066264

Barani, M., Aghaei, J., Akbari, M. A., Niknam, T., Farahmand, H., & Korpas, M. (2019). Optimal partitioning of smart distribution systems into supply-sufficient microgrids. *IEEE Transactions on Smart Grid, 10*, 2523–2533. https://doi.org/10.1109/TSG.2018.2803215

Barnes, A., Nagarajan, H., Yamangil, E., Bent, R., & Backhaus, S. (2019). Resilient design of large-scale distribution feeders with networked microgrids. *Electric Power Systems Research, 171*, 150–157. https://doi.org/10.1016/j.epsr.2019.02.012

Cagnano, A., De Tuglie, E., & Microgrids, Mancarella P. (2020). Overview and guidelines for practical implementations and operation. *Applied Energy, 258*, Article 114039. https://doi.org/10.1016/j.apenergy.2019.114039

Chalil, Madathil S., Yamangil, E., Nagarajan, H., Barnes, A., Bent, R., Backhaus, S., et al. (2018). Resilient off-grid microgrids: capacity planning and N-1 security. *IEEE Transactions on Smart Grid, 9*, 6511–6521. https://doi.org/10.1109/TSG.2017.2715074

Chen, J., Zhang, W., Li, J., Zhang, W., Liu, Y., Zhao, B., et al. (2018). Optimal sizing for grid-tied microgrids with consideration of joint optimization of planning and operation. *IEEE Transactions on Sustainable Energy, 9*, 237–248. https://doi.org/10.1109/TSTE.2017.2724583

Chen, X., Su, W., Kavousi-Fard, A., Skowronska, A. G., Mourelatos, Z. P., & Hu, Z. (2020). Resilient microgrid system design for disaster impact mitigation. *Sustainable and Resilient Infrastructure*. https://doi.org/10.1080/23789689.2019.1708176

Cheng, Y., Zhang, N., Kirschen, D. S., Huang, W., & Kang, C. (2020). Planning multiple energy systems for low-carbon districts with high penetration of renewable energy: An empirical study in China. *Applied Energy, 261*, Article 114390. https://doi.org/10.1016/j.apenergy.2019.114390

Das, L., Munikoti, S., Natarajan, B., & Srinivasan, B. (2020). Measuring smart grid resilience: Methods, challenges and opportunities. *Renewable and Sustainable Energy Reviews, 130*, Article 109918. https://doi.org/10.1016/j.rser.2020.109918

Ehsan, A., & Yang, Q. (2019). Scenario-based investment planning of isolated multi-energy microgrids considering electricity, heating and cooling demand. *Applied Energy, 235*, 1277–1288. https://doi.org/10.1016/j.apenergy.2018.11.058

Fioriti, D., Pintus, S., Lutzemberger, G., & Poli, D. (2020). Economic multi-objective approach to design off-grid microgrids: A support for business decision making. *Renewable Energy, 159*, 693–704. https://doi.org/10.1016/j.renene.2020.05.154

GAMS Development Corp. GAMS - Cutting edge modeling. GAMS (2018). https://www.gams.com/ (accessed November 1, 2020).

Gazijahani, F. S., & Salehi, J. (2017). Optimal bi-level model for stochastic risk-based planning of microgrids under uncertainty. *IEEE Transactions on Industrial Informatics, 14*, 3054–3064.

Guelpa, E., Bischi, A., Verda, V., Chertkov, M., & Lund, H. (2019). Towards future infrastructures for sustainable multi-energy systems: A review. *Energy, 184*, 2–21. https://doi.org/10.1016/j.energy.2019.05.057

Hamad, A. A., Nassar, M. E., El-Saadany, E. F., & Salama, M. M. A. (2019). Optimal configuration of isolated hybrid AC/DC microgrids. *IEEE Transactions on Smart Grid, 10*, 2789–2798. https://doi.org/10.1109/TSG.2018.2810310

Hanna, R., DIsfani, V. R., Haghi, H. V., Victor, D. G., & Kleissl, J. (2019). Improving estimates for reliability and cost in microgrid investment planning models. *Journal of Renewable and Sustainable Energy, 11*. https://doi.org/10.1063/1.5094426

Husein, M., & Chung, I. Y. (2018). Optimal design and financial feasibility of a university campus microgrid considering renewable energy incentives. *Applied Energy, 225*, 273–289. https://doi.org/10.1016/j.apenergy.2018.05.036

Hussain, A., Bui, V. H., & Kim, H. M. (2019). Microgrids as a resilience resource and strategies used by microgrids for enhancing resilience. *Applied Energy, 240*, 56–72. https://doi.org/10.1016/j.apenergy.2019.02.055

ISO-NE. ISO new england - real-time maps and charts (2015).;2015. http://www.iso-ne.com/isoexpress/ (accessed February 25, 2020).

Jacob, A. S., Banerjee, R., & Ghosh, P. C. (2018). Sizing of hybrid energy storage system for a PV based microgrid through design space approach. *Applied Energy, 212*, 640–653. https://doi.org/10.1016/j.apenergy.2017.12.040

Jimada-Ojuolape, B., & Teh, J. (2020). Surveys on the reliability impacts of power system cyber–physical layers. *Sustainable Cities and Society, 62*, Article 102384. https://doi.org/10.1016/j.scs.2020.102384

Kaviani, R., & Hedman, K. W. (2019). A detection mechanism against load-redistribution attacks in smart grids. *IEEE Transactions on Smart Grid*. https://doi.org/10.1109/tsg.2020.3017562

Khayatian, A., Barati, M., & Lim, G. J. (2018). Integrated microgrid expansion planning in electricity market with uncertainty. *IEEE Transactions on Power Systems, 33*, 3634–3643. https://doi.org/10.1109/TPWRS.2017.2768302

Khodaei, A. (2017). Provisional microgrid planning. *IEEE Transactions on Smart Grid, 8*, 1096–1104. https://doi.org/10.1109/TSG.2015.2469719

Kiptoo, M. K., Adewuyi, O. B., Lotfy, M. E., Senjyu, T., Mandal, P., & Abdel-Akher, M. (2019). Multi-objective optimal capacity planning for 100% renewable energy-based microgrid incorporating cost of demand-side flexibility management. *Applied Sciences, 9*, 3855. https://doi.org/10.3390/app9183855

Kumar, J., Suryakiran, B. V., Verma, A., & Bhatti, T. S. (2019). Analysis of techno-economic viability with demand response strategy of a grid-connected microgrid model for enhanced rural electrification in Uttar Pradesh state, India. *Energy, 178*, 176–185. https://doi.org/10.1016/j.energy.2019.04.105

Li, Z., Shahidehpour, M., Aminifar, F., Alabdulwahab, A., & Al-Turki, Y. (2017). Networked microgrids for enhancing the power system resilience. *Proceedings of the IEEE*. https://doi.org/10.1109/JPROC.2017.2685558

Li, Z., Shahidehpour, M., & Aminifar, F. (2017). Cybersecurity in distributed power systems. *Proceedings of the IEEE*. https://doi.org/10.1109/JPROC.2017.2687865

Lorestani, A., Gharehpetian, G. B., & Nazari, M. H. (2019). Optimal sizing and techno-economic analysis of energy-and cost-efficient standalone multi-carrier microgrid. *Energy, 178*, 751–764.

Ma, T., Wu, J., Hao, L., Lee, W.-. J., Yan, H., & Li, D. (2018). The optimal structure planning and energy management strategies of smart multi energy systems. *Energ, 160*, 122–141. https://doi.org/10.1016/j.energy.2018.06.198

Manshadi, S. D., & Khodayar, M. E. (2015). Resilient operation of multiple energy carrier microgrids. *IEEE Transactions on Smart Grid, 6*, 2283–2292. https://doi.org/10.1109/TSG.2015.2397318

Mansouri, S. A., Ahmarinejad, A., Ansarian, M., Javadi, M. S., & Catalao, J. P. S. (2020). Stochastic planning and operation of energy hubs considering demand response programs using Benders decomposition approach. *International Journal of Electrical Power & Energy Systems, 120*, Article 106030.

Mashayekh, S., Stadler, M., Cardoso, G., Heleno, M., Madathil, S. C., Nagarajan, H., et al. (2018). Security-constrained design of isolated multi-energy microgrids. *IEEE Transactions on Power Systems, 33*, 2452–2462. https://doi.org/10.1109/TPWRS.2017.2748060

Meena, N. K., Yang, J., & Zacharis, E. (2019). Optimisation framework for the design and operation of open-market urban and remote community microgrids. *Applied Energy, 252*, Article 113399. https://doi.org/10.1016/j.apenergy.2019.113399

Mishra, D. K., Ghadi, M. J., Azizivahed, A., Li, L., & Zhang, J. (2021). A review on resilience studies in active distribution systems. *Renewable and Sustainable Energy Reviews, 135*, Article 110201. https://doi.org/10.1016/j.rser.2020.110201

Mishra, S., Anderson, K., Miller, B., Boyer, K., & Warren, A. (2020). Microgrid resilience: A holistic approach for assessing threats, identifying vulnerabilities, and designing corresponding mitigation strategies. *Applied Energy, 264*, Article 114726. https://doi.org/10.1016/j.apenergy.2020.114726

Mohseni, S., Brent, A. C., & Burmester, D. (2019). A demand response-centred approach to the long-term equipment capacity planning of grid-independent micro-grids optimized by the moth-flame optimization algorithm. *Energy Conversion and Management, 200*, Article 112105. https://doi.org/10.1016/j.enconman.2019.112105

Mohseni, S., & Moghaddas-Tafreshi, S. M. (2018). A multi-agent system for optimal sizing of a cooperative self-sustainable multi-carrier microgrid. *Sustainable Cities and Society, 38*, 452–465. https://doi.org/10.1016/j.scs.2018.01.016

Molavi, A., Shi, J., Wu, Y., & Lim, G. J. (2020). Enabling smart ports through the integration of microgrids: A two-stage stochastic programming approach. *Applied Energy, 258*, Article 114022. https://doi.org/10.1016/j.apenergy.2019.114022

Nagapurkar, P., & Smith, J. D. (2019). Techno-economic optimization and social costs assessment of microgrid-conventional grid integration using genetic algorithm and artificial neural networks: A case study for two US cities. *Journal of Cleaner Production, 229*, 552–569. https://doi.org/10.1016/j.jclepro.2019.05.005

Nejabatkhah, F. (2018). Optimal design and operation of a remote hybrid microgrid. *CPSS Transactions on Power Electronics and Applications, 3*, 3–13. https://doi.org/10.24295/CPSSTPEA.2018.00001

Nojavan, S., Majidi, M., & Esfetanaj, N. N. (2017). An efficient cost-reliability optimization model for optimal siting and sizing of energy storage system in a microgrid in the presence of responsible load management. *Energy, 139*, 89–97. https://doi.org/10.1016/j.energy.2017.07.148

Olsen, D. J., Zhang, N., Kang, C., Ortega-Vazquez, M. A., & Kirschen, D. S. (2018). Planning low-carbon campus energy hubs. *IEEE Transactions on Power Systems, 34*, 1895–1907.

Pan, G., Gu, W., Wu, Z., Lu, Y., & Lu, S. (2019). Optimal design and operation of multi-energy system with load aggregator considering nodal energy prices. *Applied Energy, 239*, 280–295. https://doi.org/10.1016/j.apenergy.2019.01.217

Pazouki, S., Haghifam, M. R., & Moser, A. (2014). Uncertainty modeling in optimal operation of energy hub in presence of wind, storage and demand response. *International Journal of Electrical Power & Energy Systems, 61*, 335–345. https://doi.org/10.1016/j.ijepes.2014.03.038

Pecenak, Z. K., Stadler, M., Mathiesen, P., Fahy, K., & Kleissl, J. (2020). Robust design of microgrids using a hybrid minimum investment optimization. *Applied Energy, 276*, Article 115400. https://doi.org/10.1016/j.apenergy.2020.115400

Prathapaneni, D. R., & Detroja, K. P. (2019). An integrated framework for optimal planning and operation schedule of microgrid under uncertainty. *Sustain Energy, Grids Network, 19*, Article 100232. https://doi.org/10.1016/j.segan.2019.100232

Rosales-Asensio, E., de Simón-Martín, M., Borge-Diez, D., Blanes-Peiró, J. J., & Colmenar-Santos, A. (2019). Microgrids with energy storage systems as a means to increase power resilience: An application to office buildings. *Energ, 172*, 1005–1015. https://doi.org/10.1016/j.energy.2019.02.043

Senemar, S., Rastegar, M., Dabbaghjamanesh, M., & Hatziargyriou, N. D. (2019). Dynamic structural sizing of residential energy hubs. *IEEE Transactions on Sustainable Energy, 11*, 1236–1246.

Senemar, S., Seifi, A. R., Rastegar, M., & Parvania, M. (2020). Probabilistic optimal dynamic planning of onsite solar generation for residential energy hubs. *IEEE Systems, 14*, 832–841. https://doi.org/10.1109/JSYST.2019.2901844

Stevanoni, C., De Greve, Z., Vallee, F., & Deblecker, O. (2019). Long-term planning of connected industrial microgrids: A game theoretical approach including daily peer-to-microgrid exchanges. *IEEE Transactions on Smart Grid, 10*, 2245–2256. https://doi.org/10.1109/TSG.2018.2793311

U.S Energy Information Administration. (2016). Henry hub natural gas spot price (Dollars per Million Btu). *Eia*, 1. https://doi.org/10.1016/j.ijsu.2016.05.072

Venkataramanan, V., Srivastava, A. K., Hahn, A., & Zonouz, S. (2019). Measuring and enhancing microgrid resiliency against cyber threats. *IEEE Transactions on Industry Applications, 55*, 6303–6312. https://doi.org/10.1109/TIA.2019.2928495

Wang, C., Yan, J., Marnay, C., Djilali, N., Dahlquist, E., Wu, J., et al. (2018). Distributed energy and microgrids (DEM). *Applied Energy, 210*, 685–689. https://doi.org/10.1016/j.apenergy.2017.11.059

Wang, Y., Rousis, A. O., & Strbac, G. (2020). On microgrids and resilience: A comprehensive review on modeling and operational strategies. *Renewable and Sustainable Energy Reviews, 134*, Article 110313. https://doi.org/10.1016/j.rser.2020.110313

Wei, J., Zhang, Y., Wang, J., Cao, X., & Khan, M. A. (2020). Multi-period planning of multi-energy microgrid with multi-type uncertainties using chance constrained information gap decision method. *Applied Energy, 260*, Article 114188. https://doi.org/10.1016/j.apenergy.2019.114188

Wu, D., Ma, X., Huang, S., Fu, T., & Balducci, P. (2020). Stochastic optimal sizing of distributed energy resources for a cost-effective and resilient Microgrid. *Energy, 198*, Article 117284. https://doi.org/10.1016/j.energy.2020.117284

Wu, X., Wang, Z., Ding, T., Wang, X., Li, Z., & Li, F. (2019). Microgrid planning considering the resilience against contingencies. *IET Generation, Transmission & Distribution, 13*, 3534–3548. https://doi.org/10.1049/iet-gtd.2018.6816

Xie, H., Teng, X., Xu, Y., & Wang, Y. (2019). Optimal energy storage sizing for networked microgrids considering reliability and resilience. *IEEE Acces, 7*, 86336–86348. https://doi.org/10.1109/ACCESS.2019.2922994

Yang, D., Jiang, C., Cai, G., Yang, D., & Liu, X. (2020). Interval method based optimal planning of multi-energy microgrid with uncertain renewable generation and demand. *Applied Energy, 277*, Article 115491. https://doi.org/10.1016/j.apenergy.2020.115491

Yuan, C., Illindala, M. S., & Khalsa, A. S. (2017). Co-optimization scheme for distributed energy resource planning in community microgrids. *IEEE Transactions on Sustainable Energy, 8*, 1351–1360.